Rain, rock-moisture dynamics, and the rapid response of perched groundwater in weathered, fractured argillite underlying a steep hillslope

Rohit Salve[1], Daniella M. Rempe[2], and William E. Dietrich[2]

[1]Earth Sciences Division, Lawrence Berkeley National Laboratory

[2]Earth and Planetary Sciences, University of California, Berkeley

Abstract

Various field studies have concluded that shallow groundwater in weathered bedrock underlying hillslopes can contribute to both base and storm flow, and, thus, dominate runoff. The processes associated with recharge from the ground surface, through this unsaturated zone have received little study, yet they influence runoff dynamics, the chemical evolution of water, and moisture availability. Here, we use five measurement systems to document soil- and rock-moisture dynamics within a 4000 m^2 zero-order basin in which all runoff occurs through weathered argillite. At this site, the weathered bedrock zone (in which the groundwater fluctuates by 8 m seasonally) varies in depth from ~4 m at the base of the hillslope to nearly 19 m near the hill top. An aggregate-rich, porous, 0.5 m thick soil overlies the weathered bedrock. We find that during the first rains of the wet season, water rapidly travels meters into the weathered bedrock zone. Consistently, however, groundwater at some places responds quickly to the first major storm, well before the wetting front has been detected much beyond about one meter. Furthermore, throughout the wet season, the lower portion of the unsaturated weathered bedrock shows little or no moisture change. These observations suggest a fracture-dominated flow path, leading to highly variably groundwater response across the hillslope for a given storm. Seasonal changes in rock-moisture content is greatest in the first 5 to 10 m depth and may exceed the magnitude of moisture changes in the soil, suggesting that it could constitute a significant unmapped moisture reservoir.

1. Introduction

Hillslopes underlain by bedrock commonly have a mantle of soil and a variably weathered bedrock zone above the underlying fresh bedrock. In such landscapes, storm runoff is usually assumed to occur either as overland flow (Horton overland flow or saturation overland flow) or as shallow subsurface stormflow [sensu *Dunne, 1978*] in which the storm waters are perched at the soil-bedrock boundary (giving rise to relatively rapid runoff compared to deeper groundwater flow). Some have emphasized the topography of this soil-bedrock interface as a major control on runoff paths and dynamics [e.g., *Freer et al., 1997*; *McDonnell, 1990*; *McGlynn et al., 2002*; *Burns et al., 2003*]. Hillslope runoff models often treat the soil-bedrock boundary as essentially impermeable, or assign such a rapid decline in saturated conductivity with depth that this boundary effectively becomes a barrier [*Kampf and Burges, 2007*]. Widely used models for predicting the spatial pattern of elevated pore pressures and slope instability due to rain typically employ the assumption of a perched water table at the soil-bedrock boundary [e.g., *Montgomery and Dietrich, 1994*; *Pack et al., 1998*; *Rosso et al., 2006*]. While the assumption of impermeable or low-permeability bedrock underlying a conductive soil has often been employed, it has rarely been demonstrated in field measurements.

The relatively few field studies that have drilled into the weathered bedrock zone beneath the soil on hillslopes document significant storm runoff through this zone. Table 1 summarizes six such studies, which report that the fraction of runoff that travelled through the bedrock ranges from 14 to 95%. Several other studies have recently been reported that argue for significant storm flow in both fresh fractured bedrock that returns towards the surface and in weathered bedrock itself [e.g., *Banks et al., 2009*; *Shand et al., 2007*]. This runoff path matters. Deep response can be sufficiently rapid that flow through the weathered bedrock zone can dominate the storm-driven runoff hydrograph [e.g., *Montgomery et al., 1997*]. The chemical evolution of water as it travels downslope will depend on whether it travels through the bedrock or soil [e.g., *Anderson and Dietrich, 2001*; *Legout et al., 2007*]. Heterogeneities in the conductivity field of the weathered bedrock zone can lead to exfiltration gradients back [*Montgomery et al., 1997*] into the soil [e.g., *Wilson and Dietrich, 1987*; *Montgomery et al., 1997*; *Banks et al., 2009*; *Shand et al., 2007*]. This water return to the soil mantle contributes to the

generation of: (1) saturation overland flow [; *Wilson and Dietrich, 1987*; *Wilson et al., 1989*], (2) development of a subsurface variable source area [e.g. *Anderson et al., 1997*], and (3) elevated pore pressures that may lead to slope instability e.g. *Wilson and Dietrich, 1987*; *Montgomery et al., 1997* ; *Katsura, et al., 2008*; *Kosugi et al., 2008Montgomery et al., 2009*].

To generate deep, rapid runoff on hillslopes, precipitation must transit an unsaturated zone of meters to 10's of meters, and do so sufficiently quickly to cause rapid groundwater response and delivery to bordering streams. This is a problem of recharge, and as [*Gburek and Folmar, 1999*] discuss, recharge processes at the hillslope scale have received relatively little mechanistic field study. Recharge studies and theory development, typically not at the hillslope scale, have often been motivated by contaminant transport concerns, and these typically raise the issue of which has more influence, fracture or matrix flow [e.g. *Duke et al., 2007* and references therein; *Faybishenko et al., 2005*]. We are not aware, however, of any general empirical or theoretical guidelines to estimate under what circumstances rapid recharge through the vadose zone and subsurface runoff through the weathered bedrock zone predominates on hilly landscapes. Nonetheless, we can anticipate that hydrologic properties will vary strongly with rock type (and its tectonic history) and rates of erosion. Coarse-grained, quartz-rich igneous and metamorphic rocks, for example, tend to produce a sandy saprolite (where erosion rates are sufficiently slow) over a fractured bedrock where physical erosion rates are sufficiently slow. In such materials, fast and slow flow paths may still exist, although recharge may be matrix (slow path) dominated [*Legout et al., 2007*]. Recharge in chalk landscapes is often found to be matrix flow dominated [e.g., *Ireson et al., 2009*]. The runoff in the weathered bedrock zone in sandstones and shales may be fracture-network dominated [e.g.*Gburek and Urban, 1990*; *Montgomery et al., 1997*; *Heppner et al., 2007*] but little is known about recharge processes through the vadose zone of such rocks [e.g., *Heppner et al., 2007*; *Nimmo, 2010*]. Weathering and pedogenisis can effectively reduce recharge through the underlying fractured weathered bedrock and induce a shallow storm runoff zone [e.g., *McKay et al., 2005*].

The few recharge and runoff studies (cited above) on hillslopes underlain by weathered and fractured bedrock have typically relied on tracer, piezometric and water table measurements to infer process mechanisms. The unsaturated flow zone from the soil-weathered bedrock boundary to the perched water table in the underlying fresh bedrock has, however, received little direct study. This zone presents significant challenges for mechanistic investigations. It can be quite deep (over 20 m) and is really only accessible for direct measurement via drilled holes. Installation of conventional soil-moisture and tension measurement devices will not work in fractured bedrock. Geophysical methods (e.g., ground penetrating radar and electrical resistivity) tend to be difficult to interpret with regard to quantitative measures of moisture dynamics without direct independent observations in the subsurface, especially for weathered, fractured bedrock [e.g., *Reynolds, 2011*]

In order to explore the recharge process through a deep, weathered bedrock zone in a strongly seasonal rainfall environment, we use five different methods to document the early rainy season and annual rock-moisture dynamics along a steep Northern California hillslope underlain by a thick zone of unsaturated weathered and fractured argillite. The weathered bedrock zone varies across landscapes, so we tackle the entire hillslope (effectively a small zero-order basin) rather than focus on a single intensively monitored site on a hillslope. All runoff to the channel at the base of the hillslope occurs via groundwater flow that is perched on underlying low-permeability fresh bedrock, hence the recharge process to this perched groundwater is key to understanding runoff generation.

Here we first report our findings that after a long summer dry season, the first rains rapidly penetrate through the soil mantle and into the underlying weathered bedrock. Large rains generate a response as deep as 6 m into the weathered bedrock within a few weeks. But within hours to days of the start of rain, the perched groundwater, at depths from 4 to 18 m below the surface, responds. We then report analysis of seasonally moisture dynamics in which we distinguish soil moisture from *rock moisture* (a term we propose to include both exchangeable matrix water and fracture water) and find that while the soil moisture dynamically rises and falls with each successive storm event, the rock moisture in the shallow, weathered bedrock tends to

vary less after initial wet up. We conclude by proposing that rock moisture and groundwater dynamics observations strongly suggests that fracture flow plays a predominant role in transmitting water to the water table, and hence, the runoff characteristics, water chemistry, rock-moisture availability to vegetation, and the hillslope stability are all tied to this process.

2. Study Site

The focus of this study is a steep hillslope in coastal Mendocino County, in northern California (Figure 1). The site, referred to as Rivendell, is on a north facing, ~32 degree, unchanneled valley, located about 150 miles north San Francisco, within the 17 km^2 Elder Creek watershed in the Angelo Coast Range Reserve (http://angelo.berkeley.edu/). The unchanneled valley drains a surface watershed area that is about 125 m long, with a maximum width of 40 m. The site extends from Elder Creek (at 392 m asl) to 470 m asl at the ridge. Most of the site is underlain by a nearly vertically dipping argillite, the strike of which is approximately parallel to the fall line of the hillslope. Along the eastern divide, a prominent sandstone interbed is exposed at the surface. Minor interbeds of sandstone in this marine turbidite sequence are common. The bedrock is in the Coastal Belt of the Franciscan Complex [*McLaughlin et al., 2000*], which has undergone intense tectonic deformation, but retains mappable bedding (unlike the Central Belt mélange farther to the east). Incision rate along Elder Creek during the Holocene has been about 0.2 mm/yr, while Pleistocene erosion rates associated with wetter conditions approached 0.4 mm/yr [*Fuller et al., 2009*].

The Angelo Coast Range Reserve has a Mediterranean type climate characterized by warm dry summers and cool wet winters. It receives on average 1900 mm of rain annually with little snow, and there is significant variability in total annual precipitation. The bulk of the annual precipitation is restricted to a 5–6 month period in the winter. Typically, in early October, daily average temperatures at the site fluctuate around ~10^0C and then decrease close to zero by the end of December, before increasing to ~20^0C in early August (http://angelo.berkeley.edu/). Daily fluctuations in temperature are much larger during the warm summer months than in the winter. The hillslope is forested and has a limited understory. There are more than 30 Douglas fir (*Pseudostuga menziesii)*

trees that are >25 m tall within or adjacent to the surface drainage area delineated in Figure 1, with some older trees >60 m. These mature conifers are separated by a variety of lower canopy trees—e.g., interior live oak *(Quercus wislizeni*, tan-bark oak (*Notholithocarpus densiflorus)* madrone *(Arbutus menziesii)*, and California Bay laurel (*Umbellularia californica*)—creating a relatively dense vegetated hillslope. Some relatively young redwood trees *(Sequoia sempervirens)* are also present. There is no dense ground cover.

The Rivendell study site is the focus of investigation of the University of California Keck HydroWatch group and members of the National Center for Earth-surface Dynamics. Over 700 separate instruments are recording climate variables, sapflow, moisture, and water-level dynamics across the site, with over 100 million data points collected between 2007 and May 2012. The entire system is powered only by solar cells, yet, using radios, is directly connected to the internet, such that data are downloaded to Berkeley every 4 hours. Many studies are under way, including those on sap flow, transpiration rates, and influence on climate [*Link et al., 2011*], the influence of plants on atmospheric water vapor [*Simon et al., 2010*], the source water for tree transpiration and the mechanisms of rapid storm runoff and [*Oshun et al., 2010]*, geochemical evolution of runoff water [*Kim et al., In Press*], and evolution of the weathering front [*Rempe et al., 2010*]. Here, we focus on documenting, for the first time, the dynamics of the deep unsaturated zone.

3. Methods

In September 2007, seven holes (7.6 cm in diameter, 8.8 to 26.6 m in length) were drilled with a dry auger system into the hillslope using a tractor-mounted rig on and above a dirt access road and a hand-portable system below the road on the steeper portion of the hillslope (Figures 1 and 2). Periodically, a standard 140 pound (63.5 kg) weight was dropped 30 inches (760 mm) and the number of such blow counts per a unit distance advance was recorded as a metric of changing rock properties. Core was captured as a consequence of these blow count tests. A combination of high resistance to drilling, a large increase in blow counts to advance the core, and a visible absence of oxidized iron

staining was used to define the transition to fresh bedrock. All seven holes were drilled to, and in most cases, well past the weathered-fresh bedrock transition.

The drilled holes were lined with perforated PVC (polyvinyl chloride) pipes, sealed at the surface with a cement grout, and fitted with submersible pressure transducers to monitor the height of water in each borehole. These vertical holes were also used to monitor rock-moisture changes using a neutron probe (Model CPN 503DR Hydroprobe). In our surveys, we lowered the probe at 0.3 m intervals throughout the entire length of the well (including below the water table). The neutron probe is most reliably interpreted in terms of quantitative moisture content by noting successive changes at the same location with time, i.e., it provides accurate relative moisture changes [*Long and French, 1967*]. The neutron probe records water content outward from the probe about 30 cm, so local conditions around the well will prevail. Here, we report data from neutron probe surveys taken down each well at various times throughout the year. Data collected prior to May 2010 are reported in raw neutron counts because standard counts were not measured. To assess relative changes in moisture content for data collected after May 2010, the raw counts are converted to moisture content using a probe-specific manufacturer calibration. The manufacturer calibration, rather than a soil specific calibration, was considered adequate because we focus on relative changes rather than absolute measurements of moisture content. To calculate the approximate volume of water lost or gained, we assumed that the change in volumetric moisture content occurred over the entire measurement spacing of 0.3 m.

At the base of the hillslope, a differential pressure transducer was placed in Elder Creek to monitor water level variation. Approximately 150 m upstream along Elder Creek, a United States Geological Survey benchmark real-time gauging station has operated since 1965 (Station 11475560).

To observe moisture-content changes in the shallow vadose zone into the weathered bedrock, i.e., up to a depth of ~2 m, we used time domain reflectometer (TDR) probes, (TDR100, Campbell Scientific) and Electrial Resistance Sensory Array System (ERSAS). Time domain reflectometry TDR installation in bedrock, requires special methods to avoid gaps between the probes and the rock [*Sakaki and Rajaram, 2006*], and such measures are difficult to employ when attempting to define moisture dynamics by

inserting probes in vertically drilled holes. An alternative would be to dig trenches, but the disturbance was considered too great to do this extensively across the study area. Instead, each hole was instrumented with 4 to 5 TDR probes (0.30 m long), installed vertically (Figure 3a). TDR probes within the soil layer were backfilled with native soil, while those below the soil-weathered bedrock interface were installed in silica flour. The probes were isolated with a ~0.05 m thick layer of powdered bentonite to prevent vertical movement of water within the backfilled holes. It is important to note that measuring the water content of silica flour does not indicate the water content of the natural material, because equilibration between the two occurs on the basis not of water content but of matric potential. As such while the silica flour provided an excellent medium to monitor first wet up, it clearly has very different water-retention properties than the surrounding weathered, fractured bedrock, and the flour-embedded probes reveal little about storm dynamics or absolute moisture content in the surrounding bedrock.

To improve the record of moisture dynamics in the soil, we dug trenches (<0.75 m deep) at 6 locations and installed 0.075 m long TDR probes horizontally at 3 and 8 depths (a total of 34 probes) to document the moisture dynamics in the soil and shallow saprolite where probes could be pushed into the material easily. Trenches were backfilled with excavated material. The vertically oriented TDR series is referred to as the S series, whereas the horizontally oriented probes are referred to as the T series. Dielectric measurements were converted to volumetric moisture content (for the probes in the native soil) using the Topp equation [*Topp et al., 1980*] which has been shown to be accurate within a few percent for a wide variety of soils [*Dalton, 1992*] and has eliminated the need for soil-specific calibrations for most routine applications [*Ghezzehei, 2008*].

The ERSAS consist of a vertical array of sensors (spaced every 10 cm) . Each sensor, includes two electrical leads located between pieces of Watman's filter paper (Figure 3c). Electrical resistance changes, as a consequence of moisture variation, are measured across the sensor [*Salve, 2011*]. The sensors are mounted on a thin strip (0.02 m wide) of PVC (Figure 3c). The PVC strip was pushed against the borehole wall such that the probes were in immediate contact with the formation. Once the PVC was installed, the borehole was filled with silica flour to prevent the probes from losing contact with the formation. This method ensures a close contact between the paper and

surrounding material, and provides a highly sensitive indicator of first arrival of moisture at depth with the first rains in the fall. [*Salve, 2011*] describes in detail the construction of these devices and initial testing, concluding that the system successfully detects the timing of moisture change (although somewhat more slowly than TDR), and that the relative amount of resistance detected in the filter paper does correspond qualitatively to the relative amount of moisture in the material in contact with the filter. No conversion algorithm from resistance to moisture is proposed, so we use the system to record timing and apparent relative magnitude of moisture change. Both the ERSAS and TDR methods are temperature sensitive, and in addition, the ERSAS measurements will vary with soil solution chemistry. As will be seen, these effects are relatively minor compared to changes induced by seasonal moisture changes.

The TDR probes that extended into the weathered bedrock and the ERSASs were installed in eight pairs of vertical holes, each ~2.0 m deep, augured at three elevations along the hillslope (Figure 1). The TDR probes in the six shallow profiles only in the soil (T-series) were located in close proximity to the S series probes and ERSAS profiles. The data from the probes were recorded every 15 minutes from 2007 to mid 2009, and every 5 minutes since 2009, providing accurate timing of arrival of the wetting front with depth. Note that despite the seeming fragility of the ERSASs, they have functioned continuously for 5 years as of the time of this writing.

Thirty soil-moisture probes (SM200, Dynamax, Inc.) were installed to a depth of about 20 cm along the three levels. The SM200 probes measure the permittivity of the formation, which can then be converted to a value of moisture content. These probes progressively failed through the monitoring period, but provided clear initial observations on moisture dynamics and gave critical empirical support to the use of the ERSAS sensors.

The microclimate of the hillslope was monitored with four rain-gauges (TE525 Campbell Sci., Inc), three temperature and relative humidity probes (Model HMP 45C, Campbell Sci., Inc), and a barometric probe (Model PTB100B) (Figure 1). Microclimate data were also recorded in an open meadow across Elder Creek from the site (initiated in Fall 2008 using the same system as on the site) and in a meadow location 1.5 km to the south at the Angelo Coast Range Reserve Headquarters (the two meadow readings were

nearly identical so we report just the data from the nearest one to the study site) Measurements from the TDR probe were made with a reflectometer (Model TDR100). Seven control devices (CR1000, Campbell Sci.,) were used to monitor all sensors located along the hillslope. The clocks on the control device were synchronized and periodically checked to ensure that timing of measurements along the site were always consistent.

During the four-year period of monitoring between September 2007 and August 2011, we evaluated the hydrologic response to rainfall both within and between seasons. As the hillslope responded to individual events, we were able to compare recharge dynamics in the shallow, near-surface materials with that of the deeper, unsaturated fractured rock zone. We also evaluated the longer-term seasonal moisture-content changes in the fractured rock zone. Specifically, we documented: (1) the unsaturated zone response to the first storms of the season, (2) the response time of individual wells to individual rainfall events, and (3) temporal trends in response time and moisture storage within weathered bedrock zone. Response time was defined as the duration between the start of a precipitation event and the first response observed at a particular location, while lag time was defined as the time difference between the peak rainfall and peak response (Figure 4). Time of first response was most difficult to identify in the creek and groundwater levels. In some cases, due to background variation, we concluded we could not clearly identify a first response time. The rain gauge data in the open meadow were used as the reference rainfall record for these analyses. The first-year data were not used because of some uncertainties associated with the precipitation measurements in Year 1 and delayed installation of some equipment. A storm was defined as a period that exceeded 2 mm of rain after more than 6 hours of no rain.

While most observations from this investigation (i.e., precipitation, atmospheric temperature, moisture-content changes in shallow profile, water table fluctuations) are from continuous measurements made at a high temporal resolution (initially 30–60 minutes, but in later years 5 minutes), the single exception, neutron probe measurements of moisture-content changes in the fractured rock, are from periodic measurements made at various intervals over two years.

4. Observations

4.1 The weathered zone

A thin mantle of stony soil (typically less than 50 cm) blankets the argillite. The National Resources Conservation Service maps the area as part of the Yellowhound-Woodin-Ornbaun complex [*Soil Survey Staff, Natural Resources Conservation Service, United States Department of Agriculture, Web Soil Survey*]. These are described as gravelly, well-drained soils developed on sandstone, shale, and conglomerate. We find that the A horizon (~20 cm) is intensively woven with roots that extend throughout the profile and into the underlying saprolite and weathered bedrock. Small holes, left from burrows and decayed roots, are common. No continuous cracking has been observed, in strong contrast to the underlying saprolite and weathered bedrock. The depth extent of the weathered argillite beneath the soil varied from about 4.5 m near the base on the hillslope (Well 1) to about 18.5 m (Well 10) in the upper part of the catchment (Figures 1 and 2). The first several meters into the zone below the soil-bedrock boundary consists of intensely shattered, weathered bedrock (saprolite) that is well oxidized along fracture surfaces. This material was easily penetrated during blow count measurements. With increasing depth, blow counts to obtain core progressively increased, until at greatest depth, penetration was essentially stopped. Degree of oxidization and frequency of open fractures also decreased with depth. The fresh, dense, resistant bedrock at the base of each hole lacked evidence of oxidation. Although these rocks have undergone intense tectonic deformation, the fracture system in the fresh bedrock at depth appears to be tight. Field observations of river gravels and simple laboratory trials show that the moist argillite quickly shatters upon drying; hence, we hypothesize that much of the shattering of the bedrock in the weathered zone is associated with wetting and drying cycles, with only minor chemical losses [*Rempe et al., 2010*]. Thus, although spatially heterogeneous, in general the weathered bedrock zone grades with increasing depth from relatively soil-like granular material to low-permeability bedrock bounded by fractures, whose frequency and openness of apertures decline with depth until reaching fresh bedrock. The strike of the nearly vertically bedding of the argillite is nearly parallel to the maximum fall direction. This may introduce systematic permeability contrasts associated with bedding features across the hillslope.

4.2 Precipitation

At the two meadow sites, the rainfall differed by less than 2% for the three years 2008–2010. Two of the hillslope rain gauges under the forest canopy operated continuously in 2009 and 2010, and the ratio of under-canopy annual rainfall to meadow rainfall varied only from 0.73 to 0.75. Two rain gauges cannot be expected to give a reliable indication of interception rates, but this ratio is remarkably close to the interception rate of 22% reported by [*Reid and Lewis, 2009*] in a nearby second growth redwood forest and to the 22% proposed for needle trees globally [*Miralles et al., 2010*]. The rainfall intensities for individual storms were often very similar between the meadow and under the canopy; hence, the meadow record provides a good input data set for site response analysis.

The number of rainfall events at the meadow site increased each year, as did the annual rainfall (Table 2), with the final two years close to the estimated average annual rainfall. Peak runoff exceeded the 1.5-year recurrence interval discharge (11 m^3/s) only three times within the monitoring period. The maximum observed discharge in Elder Creek was 14.2 m^3/s in response to a 98 mm rainfall event.

Typically, there was a 3–5 day dry period between storms, although up to 31 days between storms occurred during the 2007–2008 season. Five-minute rain records rarely exceeded a rate of 10 mm/hr, and only reached 30 mm/hr for a few 5-minute intervals. Rates at 15-minute averages exceeded 10 mm/hr for two percent of the period of recorded rain. Thus, during the monitoring period, rainfall intensities were modest, consistent with the low-intensity storms that typify the Pacific West Coast, [e.g., *Bureau, 1968*]. Storms used to analyze response times and lag times ranged in duration from 0.89 days to 6.69 days, with rainfall per event ranging from 38 to 190 mm: these were above-average rainfall events.

4.3 Response to the first storm of the season

The seasonality of climate at our study site leads to a regular cycle of winter wetting and then months of no rain, during which the landscape drains and the soil and weathered bedrock zone dries (Figure 5). At the end of the dry season, the water table is close to the fresh-bedrock boundary, and the flow in the adjacent Elder Creek to which

our site drains is on the order of 0.1 mm/day. The TDR, both the S and T (just in the soil) series, and ERSAS at this time record minimal moisture content (about 7%) and show little average temporal variation. Relative air humidity dips to less than 20% during the late afternoon, but recovers to about 90% in the early morning. Though dry, the soils show no surface signs of cracking.

In each of the water years with complete data records (2008–2009, 2009–2010, 2010–2011), rain fell in mid-September for less than 24 hours and then was followed by up to one month of no rain. The September 19, 2008, precipitation was just 2 mm over 15 hours. In 2009, the September storm left 13 mm in a 4.5 hour rain event. All of the ERSAS sensors responded to depths of 10 cm; four profiles showed response below 40 cm, and one probe detected moisture increase at 90 cm below the surface (Figure 6). Four of the soil TDR profiles responded at depths of 30 cm, but two responded at 70 cm below the surface. No wells responded. The September 2010 precipitation left 19 mm in 13 hours and also caused no response in the wells. But moisture was detected by nearly all the ERSAS profiles to depths of 40 cm, and two responded at a depth of 90 cm. Some of the TDR profiles had probes that responded to depths of 30 cm, and one responded at 70 cm. These two early rain events show that locally deep penetration (up to 90 cm), well into the weathered bedrock zone, occurs with even modest rain amounts. But these storms were not large enough to cause a groundwater response. No recharge occurred. Each year, during the month following the rain, moisture progressively declined, but the wetting front did not advance to significantly greater depth. (The September rains technically fall in the previous water year.) To avoid confusion, we will refer to each year by the year in which the first fall rains (September or October) occurred—hence, 2008, 2009, and 2010.

The first major storms occurred in October of each year and were similar in magnitude and duration (Figure 7, Table 3). The 2008 storm was 96 mm over 28 hours (3.4 mm/hr average), the 2009 storm was 134 mm in 43 hours (3.1 mm/hr average) and the 2010 storm was 220 mm in 41 hours (5.4 mm/hr) (but 192 mm fell in just 21.5 hours in the heart of this storm (8.9 mm/hr)). Peak 15-minute rainfall intensities were 13 mm/hr (2008), 24 mm/hr (2009), and 29 mm/hr (2010). The rainfall varied during each storm, and in the longest (2009), there were three pulses separated by 2-hour breaks of no rain

(Figure 7). Unlike the September rain, all but two of the ERSAS sensors and 12 of the TDR S-series probes responded to the 134 mm of rain in 2009. The 220 mm of rain in 2010 caused all sensors to respond.

Figure 8 shows the depth profile of response time between the start of rain and detection of moisture increase using the ERSAS and TDR probes for two water years, from 2008 (year 2) to 2009 (year 3). Here, we use cumulative rainfall as a surrogate for both time (see cumulative rainfall plots in Figure 7) and input volume driving the response. The two systems of moisture detection reveal similar patterns, and these patterns differ along the hillslope. The probes at level 1 (Figures 1 and 8) show that early rains penetrate rapidly through the soil (< 50 cm deep) into the underlying weathered bedrock to a depth of about 1 to 1.4 m. Then, the rate of progress of wetting slows, with the deepest probes only wetting up at the end of the storm or later (in Year 2 season). The input rains in Fall 2008 and 2009 differed in the temporal sequence of rain bursts, but the concave upward profiles were similar for both years and for all three measurement sites at level 1. The concave upward profiles suggest a material property change at depth, perhaps to less broken bedrock beyond 1 m.

Level 2 (Figures 1 and 8) profiles had greater variation with depth, but also showed a rapid pulse past the soil (~50 cm) into the weathered bedrock (to the first 0.8 m based on ERSAS data), and then a slowing of the wetting advance for two of the three profile sites. Level 3 (Figures 1 and 8) profiles differ in several ways from the other two levels. Penetration rate for the first wetting response was slower, the individual profiles showed greater differences between measurement systems (TDR versus ERSAS), and among the sites, the profiles tended toward a convex up form. The convexity of form occurs in both the ERSAS and TDR data. In the case of ERSAS, data profiles at Station 1 and 3 (Figure 8), the deepest measurement points (i.e., depths close to 1.8 m), show wetting at the same time as the shallow values (i.e., depths up to ~0.4 m and well before the intermediate depths above. This would suggest that some infiltrating water is getting past the intermediate depths, presumably along concentrated preferential flow paths, without fully moistening the deeper soil and weathered bedrock.

A striking and unanticipated result is the quick well response up to 18 m below the surface to the first major-storm of the season (Table 4, Figures 7 and 8). In most

cases, the wells rose before the TDR or ERSAS at depths of greater than 1 m had detected a moisture change. Wells 5 and 6 were distinctly slower, or didn't respond to the first storm. The rainstorm of October 2008 presents the clearest results, because rain began abruptly as compared to gradually in subsequent years (Figure 7). For wells 2, 3, 7 and 10, response was just 8.5, 2.5, 3, and 8 hours into the 28-hour storm, respectively. For two wells 3 and 7, the response occurred after just 9.4 and 11 mm, respectively, of rain had fallen. This is considerably smaller than two of the September rains (2009 and 2010), when there was no response in any wells.

The response differed greatly among the wells and from year to year at the same well. Well 1 responds to level variations in Elder Creek; thus, timing and magnitude of response tells us little about rainfall response. Wells 5, 6, and 7 are on the dirt road that crosses the site. These road wells lacked a soil mantle, some of the weathered bedrock, and at peak rainfall intensities may have lost some water to runoff from the road surface. Wells 5 and 6 were distinctly slower in response, whereas well 7 (located where the cut into the hillslope is shallowest) responded rapidly, like wells elsewhere off the road. The velocity of response (depth to well divided by time to response) varied from 21 to 530 cm/hr for the 4 more dynamic wells (2, 3, 7, and 10).

The magnitude of well response to the first rains in October varied greatly among the wells and in successive years. Wells 2 and 3 consistently responded with a greater water level rise than the others. In 2008 and 2009, well response was 0.46 and 0.68 m in well 2, respectively, while it was 0.3 m and 0.7 m in well 3. In contrast, wells 7 and 10 rose just 0.09 m and 0.18 m (well 7) and 0.13 and 0.3 (well 10) for the two years. But in 2010, wells 2 and 3 rose 2.0 and 6.37 m, respectively, and wells 7 and 10 rose 0.5 and 0.55 m, respectively. Wells 5 and 6 rose very little or not at all in response to these first rainstorms.

Another measure of first response is the lag to peak from rainfall to peak well rise in the first storm. Here, we use the centroid of rainfall given the high short-term variability of rain. The lag to peak is similarly rapid and is generally faster than the response time (Table 4). Values ranged from less than an hour to 25 hours (excluding the slow response at well 6).

4.4 Soil- and rock-moisture dynamics

The combination of the ERSAS and TDR profile monitoring and neutron probe surveys enable us to quantify moisture dynamics in the soil and weathered bedrock zone. As mentioned above, here we propose to use the term *rock moisture* to refer to the bulk dynamic moisture content, which includes both the mobile moisture within the bedrock itself (often referred to as matrix water) and that moisture coating fracture surfaces and held in the apertures bounded by rock fragments and fracture walls (fracture water). Consequently, rock moisture applies to the bulk water content of rock—whether it is saprolite, weathered, or fresh from dry to a saturated state. Near the ground surface, the weathered bedrock tends to be sufficiently broken such that it has a soil-like texture and may have a water-holding capacity similar to that of soil. Rock moisture here is likely dominated by the pore space created by intense weathering. Deeper into the weathered zone, where the material condition shifts to more coherent bedrock bounded by partially open fractures, we hypothesize that changes in moisture may be dominated by water in the fractures, given the apparently low permeability of argillite.

Figure 9 shows a comparison between selected ERSAS sensors and two nearby SM200 probes (installed at about 30 cm depth) in response to precipitation during 2009–2010. The precipitation data, recorded at 15-minute intervals, are normalized by the maximum 15-minute rainfall rate of the year. The data for each ERSAS and SM200 sensor is plotted as a normalized function of that individual probe's total range of response. The shallow (0.1 and 0.2 m—thus, in the soil) ERSAS sensor responded to each rainfall event with a rapid rise followed by a progressive decline between storms, and a rapid decline at the end of the wet season. The similarity to measurements from the SM200 probes gives strong support to the use of the ERSAS to record dynamic moisture change.

Figure 10 compares the ERSAS sensor response for three representative profiles at each of the three levels from October 1, 2009, to October 1, 2010. Generally, the moisture-increase with fall rains drives the resistance to near-zero values at all sensors, but the shallower sensors showed greater resistance (less moisture) throughout the winter and dried out (larger increase in resistance) more quickly in the summer. These data strongly suggest that in contrast to the soil-moisture dynamics in the winter (Figure 9 and 10), rock moisture (in the shallow, weathered bedrock zone) tends to remain consistently high. The moisture dynamics differ systematically

with levels. The higher up along the slope (from level 1 to 3), the greater the depth of winter moisture dynamics, and the deeper the depth to strong drying (large increase in resistance) during the summer. As resistance increases with drying, so too does the noise in the data, but it is consistently more variable at shallow depths, probably due to the temperature sensitivity of the system.

Figure 11 shows the seasonal dynamic in moisture 2008–2009 at the three levels at Rivendell, as recorded by the ERSAS system and the TDR- T series probes. The data for each individual ERSAS sensors (e.g., at 0.15 m depth) is normalized by the maximum range of resistance measurement for that individual probe. The TDR moisture content uses the standard conversion from dielectric constant to moisture content, as discussed in the methods section. The TDR probes and ERSAS sensors in the soil record individual storm dynamics, reveal a progressive rise in average moisture with repeated sustained rainfall during the winter, and show a mean moisture content in the soil well below that of the underlying weathered bedrock. Both systems document the moisture content rapidly rising in the weathered bedrock, showing little response to repeated storms through the winter, and then, at the end of the rainy season, declining rapidly at first and then decreasing more slowly through the summer. This comparison further supports the utility of the ERSAS system and allows us to conclude that in Figures 9 and 10, the dampening with depth of the temporal variation in moisture, as storms sweep through, probably reflects a true dampening of moisture dynamics with depth.

To estimate the field capacity and wilting point values of the soil, we relied on the two TDR systems: the shallow T series probes located horizontally in the undisturbed soil, and the shallowest S series probe that was placed vertically in back-filled native soil. We assume that the substrate is near field capacity in May 2009 and, based on flattening of the response, reached close to wilting point by September 2009 (Figure 9). We add an additional period from July to September to focus on moisture change during this most limiting period of water demand. The two series yield somewhat different results. For the T series, the average moisture decline between May and September 2009 was 17%, and between July and September was just 2.7%, with resulting water loss of 111 mm and 17.5 mm, respectively. For the S series, the average moisture decline between May and September 2009 was 29.4%, and between July and September was 21.3%, with resulting

water loss of 130.7 mm and 103 mm respectively. For the period June 15 to September 15 2010, the water loss was 56 mm for the T series and 66 mm for the S series. The S series reports more moisture with a slower decline than the T series. The T series has the advantage of the probes being placed horizontally in undisturbed soil and provide multiple readings through the depth profile—but the probes are short, and the resulting signal is relatively noisy. The S series have longer probes, but are placed in disturbed native materials, i.e., soil back-filled into drilled holes. We propose that the T series, by preserving soil structure, may provide a better estimate of moisture, which would imply about 111 mm of summer moisture loss in the soil in 2009 and 56 mm in 2010.

Figure 12, an example of the T series measurements at level 2, shows that each depth displays a persistent moisture-level position throughout the winter. Moisture pulses associated with rain events pass rapidly through the profile (recorded every 15 minutes), but at a specific location beneath the surface, the moisture tends to hover around some particular value, with the driest the shallowest value. This was the case in 5 of the 6 T series profiles. Structured heterogeneity and fine-scale moisture-tension-conductivity relationships within the soil itself appear to dictate the moisture- depth relationships in the soil.

Between October 2008 and November 2010, we made a series of measurements in the deeper unsaturated profile, using a neutron probe. We compared measurements made between February 2009 and May 2010 to those made in October 2008 (Figure 13) by subtracting the raw neutron count from the neutron count measured on October 2008 at each particular depth. A positive change indicates moister conditions than those observed in October 28, 2008 (which was surveyed after 111 mm of fall rain and, thus after the event described in Figures 6 and 7). Between the October measurement and that in Feb 2009, 577 mm of rain had fallen. February to March measurements show that 464 mm of additional rain occurred, and then between March and April, 142 mm of rain fell. The April measurement was followed immediately by 183 mm of rain, and then no rain for about two months prior to the July 16 measurement. After the July measurement, there was a further 2 months of no rain, then starting in September, there was 190 mm of rain before the November measurement.

Figure 13 shows the moisture-change response during these successive measurements and the location of the water table at the time of measurement. The February profile is wetter than the reference October profile and, generally, the March profile is slightly wetter than February. March to April shows some weak drying, followed by strong drying by the time of the July 16 measurement. The drying is strongest in the first 3 to 5 m and much less (even absent) in the deepest portions of each profile. After July 16, there were two more months of no rain. This was followed by 190 mm of rain weeks before the November measurement appears. The drying followed by rain between July and November is recorded in the surveyed moisture profile (Figure 13). In November, well 2 was wetter (relative to July) to a depth of about 5 m. Well 3 was wetter to a depth of about 4 m, but then distinctly drier at greater depth, including having a lower water table. Well 5 was wetter only about 2 m down and then drier to about 16 m. Well 6 was wetter to nearly 4 m, but then drier to about 7.5 m. Well 10 was wetter to about 2 m, and then drier throughout the rest of the profile (with a much deeper water table. Well 7, surprisingly, shows no wetting, but instead was drier throughout the profile.

These changes strongly indicate that the first rains of fall 2009 penetrated sufficiently into the weathered rock zone to elevate moisture content detectably 2 to 5 m below the surface. This extends to greater depth than the moisture change recorded in the ERSAS and TDR systems (Figure 8). As shown in Table 4, in 2009 wells 2, 3, 6 and 10 responded to the October rains. Hence, despite no detectable change in moisture beyond 2 to 5 m, the wells responded. It is noteworthy that well 7 did not respond to the October storms and its profile remained much drier. The lowest portions of each profile showed the least amount of moisture dynamic, despite all recharge traveling through these levels—and even following complete saturation followed by lowering of the groundwater table (as indicated both by the temporal maximum water table height and the height current with measurement), the relative moisture change was small. This finding suggests very little moisture change is needed to cause saturation at depth.

Figure 14 a and b show the groundwater and rock-moisture response at well 3 to two storms that dropped a total of 260 mm (175 mm and 84 mm plus minor rainfall between the two storms) from October 10 and November 5, 2010. The groundwater rose abruptly 6.5 m in 10 hours, fell back 4.8 m over about 4 days, and then rose again 4.4 m

in 17 hours (Figure 14a). Rock moisture systematically increased down to about 4 m below the surface, adding about 186 mm to the weathered bedrock, but did not significantly change in the zone that experienced the fluctuating water table. The rock-moisture-gain profile in 2010 is similar to that of 2009 for these first rains: depth of detected change ranged from just 2 m at well 5 to 6 m at well 6 (Figure 15). Well 7, which showed no response in 2009, experienced increased rock moisture to 6 m in 2010. The average rock-moisture increase was 115 mm during this period.

One striking feature of all neutron probe profiles reported in Figure 13 is the systematic, yet heterogeneous moisture-change response with depth. Some levels showed large seasonal moisture variations, but some did not. Levels of low moisture increase tended to remain that way throughout the season. Wells 2 and 7 show greatest moisture addition at middle depths, well 10 had largest moisture increase in the first 2 m, wells 5 and 6 were relatively uniform in moisture-content change (at depths less than where virtually no changes occurred). Well 3 had the largest overall moisture-level change, which extends non-uniformly throughout the profile. Taken together, these profiles paint a picture of a structured heterogeneity, with individual well sites differing dramatically from each other in the vertical structure and magnitude of moisture-change response.

The net summer moisture loss from the weathered bedrock zone was calculated using a May 2010 neutron probe profile survey and comparing that to the October 28, 2008 reading. Since readings were not done precisely at the spring end of rain and just before start of rain in the fall, we picked the wettest late spring reading and the driest fall reading, so our numbers may represent a high number. Counts were converted to moisture (using manufacture calibration) and differences in moisture content integrated from 1 m below the surface to the full depth of each profile. The average moisture loss through the summer from this weathered bedrock zone was 138 mm (ranging from 56 to 270 mm). The spatially weighted mean is 115 mm. Despite an upslope thickening unsaturated zone (Figure 2), the total moisture content does not systematically increase upslope. The summer moisture decline in the shallow soil and the deep bedrock is comparable, although the loss occurs later in the weathered bedrock. Furthermore, this moisture loss can be gained in the first storms of the winter: the first two October storms of 2010 added 115 mm of rock-moisture storage.

A check on these moisture changes is the annual water balance of Elder Creek (Table 5). Based on field observations that show nearly complete drainage of the perched water table in the weathered rock zone by the end of summer, and the lack of permeability of the underlying fresh bedrock (thus no significant deep percolation), we assume that there is no net annual storage loses or gains on the hillslope. Annual precipitation minus runoff and interception is the seasonal moisture that is stored and removed through evaporation and transpiration. Because of the dominance of hardwoods in Elder Creek as a whole, the interception component is less than the roughly 25% that is estimated from our site measurements (and supported by literature values). We assume the watershed-scale interception to be about 13% [*Miralles et al., 2010*]. Table 5 shows the estimated evapotranspiration (ET) for three water years on Elder creek. These values suggest an ET of 300 to 500 mm per year. Summer seasonal rock- and soil-moisture loss is about 200 mm. Some of this loss may be due to continued slow recharge to the perched groundwater system. The ET on the north-facing hillslope is probably less than the basin-wide average. Furthermore, given the active transpiration at other times of the year by the forest [*Link et al., 2011*] and evaporation in the fall and spring at our site, a difference between the summer moisture loss and the annual evapotranspiration is expected. Hence, the measured annual soil- and rock-moisture loss of about 200 mm seems reasonable.

5. Discussion

5.1 Moisture dynamics and groundwater response

The five systems of moisture measurement coupled with monitoring of groundwater table dynamics across the hillslope reveal a consistent pattern of rapid influx of incoming rain to the weathered bedrock zone, a highly variable advance rate of rock-moisture increase with depth, and a rapid, but very heterogeneous groundwater response at depths over 18 m below the surface. After summer months of no rain, relatively light September precipitation nonetheless infiltrated to depths of 0.9 m at some locations on the hillslope. Subsequent first major storms in October drove water through the roughly 50 cm soil, and down to depths of 6 m into the weathered bedrock. Before this deep penetration, even relatively early in the storm event, many of the wells in the groundwater had responded, though the response magnitude varied greatly among the

wells. A doubling of the first storm intensity between 2009 and 2010 caused up to a 10-fold increase in height in the local water table, but local groundwater response varied greatly across the hillslope. Most surprisingly, at the deeper levels where the local water table rose and fell, the rock moisture before and after the water table pulse remained unchanged, and generally, the deepest unsaturated levels showed no detectable change in rock moisture over the winter season.

Moisture-content variation appears strongly tied to changes in material property with depth, and points to changing processes of water transit through the unsaturated zone. By all measures, the soil consistently showed a rapid, dynamic response to rain events, with moisture content quickly climbing in spikes of rain and then draining, leaving an average moisture content well below maximum storm values. The ERSAS data in the first storms suggest a slowing of the rate of wetting front advance as it enters the shallow weathered bedrock zone, and a dampening of response to subsequent storm pulses. We also see evidence in the first storms of fast, deep response in ERSAS data relative to shallow levels.

Soil-moisture and shallow-rock-moisture dynamics varied systematically along the hillslope (Figures 8, 10, and 11). Generally at the lower elevations, moisture content rose rapidly with first rains (slowing as moisture entered the saprolite), showed minor variation in moisture content during the winter, and then differentially dried out. Progressively upslope, the saprolite held less water in the winter and dried more deeply during the summer, suggesting that the forest more strongly drains the rock-moisture zone higher up the hillslope. Water demand on the vegetation presumably is greater up the hillslope, where it is hotter, less humid, and receives greater solar radiation.

The neutron probe data show seasonal drying of the entire weathered bedrock zone, equivalent to a loss of about 100 mm. First rains penetrate to variable depths, but typically several meters into weathered bedrock zone. Subsequent rains raise moisture levels at depths up to 10 m. In response to these first storms, the vertical profile of rock-moisture increase differed among the wells, ranging from nearly uniform with depth increase (well 2) to strongly decreasing with depth (wells 3 and 5). Flow was passed through the lower portions of these profiles with no detectable change in moisture content.

5.2 Measurement methods

The five methods we used to track moisture content are: 1) TDR with 0.3 m probes set vertically into silica flour (in the weathered bedrock zone) and disturbed native soil (for the soil layer) (referred to as the TDR S series) 2)TDR with 0.075 m long probes inserted horizontally in vertical arrays into the soil and saprolite, (referred to as the TDR T series),3) commercial SM200 soil probes, 4) the ERSAS filter paper moisture detection system, and 5) neutron probe surveys. As a standard for moisture measurements TDR is well established, however, the method requires insertion of probes into the media, and this is difficult to accomplish in weathered bedrock. The first method we tested did not work as a means to document moisture content change throughout the year: silica flour in the borehole does provide a media into which probes can be inserted, but the silica flour properties dominate over the weathered bedrock. The probes in the silica flour did, however, provide valuable data on the downward propagation of the first response to the winter rains. Backing filling the hole with disturbed native materials creates a new material quite different from the weathered rock. Backfilled native soils may be more like undisturbed, but the soil structure is lost. This led us to use the short probes inserted horizontally into the soil and saprolite. This method provides our best quantitative measure of local moisture content, but the short length of the probes increases the error. The unanticipated result of the measurements with this system is that within the soil there are local, persistent moisture differences even as rain-driven infiltration events passed through the soil. This will need further testing but has potentially important implications for understanding soil water dynamics.

The commercial probe (SM200) was least reliable, displaying drift, high temperature sensitivity, noise, and lack of durability. Nonetheless, the probe provided a reference data set early in the project, when their functionality was relatively good, to compare with the recently developed ERSAS system. This system is constructed of inexpensive materials and is easy to make. But more importantly, it provides a unique method for continuous detection of moisture changes in weathered bedrock. The filter paper can be pressed against an exposed wall of the borehole and thereby overcome the problems associated with the use of TDR in this setting. Further testing is now needed to

determine if a moisture- resistance relationship can be established to enable quantitative moisture detection. The neutron probe provided us with the key rock moisture data throughout the weathered bedrock, but we found we could not operate the probe during rainstorms without risk of damaging the instrument. It is also, now, an instrument that requires considerable persistence simply to get a permit to use it (and pay associated fees). The ERSAS would overcome both of these difficulties if the resistance measurements could be converted to moisture content

The interpretation of the well measurements can be questioned. If vertical flux during rains is largely focused along fractures, one might argue that such fractures would preferentially drain into our wells, and the quick response at depth is an artifact of the well. Such narrow vertical wells are not likely to cross or attract many strongly conducting fractures. Furthermore, the limited number of conductive fractures that are crossed by the well are unlikely to provide sufficient flow to sustain a rise against a strong tendency to drain laterally. An artifact of measurement using well observations seems very unlikely in our case.

5.3 A conceptual model

Figure 16 presents a conceptual model of moisture dynamics that points to possible mechanisms explaining the moisture dynamics and groundwater dynamics of the weathered bedrock zone. It is a 1-D model focused on infiltration processes, but lateral head gradients in the saturated zone on our steep hillslope lead to subsurface flow, and this is suggested in our illustration. The figure shows four distinct materials with depth (finer divisions could be made): a soil layer, a near-surface weathered bedrock region, a deeper weathered bedrock zone, and fresh bedrock. The soil has fine rock fragments, abundant visible biogenic macorpores and roots, and is highly conductive and quickly drains. The near-surface weathered bedrock layer is sufficiently fractured and infused with fines that, despite retaining a relict rock structure (easily visible in our road cut), the material has a soil-like appearance and can be called a saprolite. Here, we will use that term to refer to this layer. Our deep drilling revealed a progressively more resistant, less broken, and less chemically altered material with depth into the weathered bedrock zone. This weathered bedrock layer can be conceived as being composed of a blocky matrix of

argillite (with minor components of sandstone interbed) bounded by fractures of widely varying orientation, aperture width, and connectivity, the frequency of which declines with depth. We infer that the conductivity of the matrix blocks, the bulk porosity, and the amount of storage and conductivity of water along the fractures both decrease with depth. The underlying fresh bedrock is sufficiently closed such that water remains perched above it, and it remains saturated throughout the year. The fresh bedrock effectively bounds the hydrologic system.

In Figure 16, the first profile represents the fall period after up to 6 months of little or no rain: the soil, saprolite, and weathered bedrock zone have reached low, nearly constant soil and rock-moisture levels. Moisture levels in the soil are reduced to about 5% (Figure 11). The water table generally remains perched on the fresh bedrock and is still slowly receding, as it drains to the Elder Creek, thereby contributing to sustained base flow throughout the summer. We note that collaborative research on the site indicates that by the fall, although sap flow and thus transpiration rates in vegetation have declined, they are still active—consequently, moisture is still being drawn down [*Link et al., 2011*]. We cannot yet say, however, how deeply rock moisture is being extracted by overlying trees, nor how much of the summer decline in rock moisture at great depths in the unsaturated weathered bedrock zone is caused by slow, continuous drainage to the water table.

The first major storm of the season (typically in October) injects water through the soil, into the saprolite, and if the storm is sufficiently large, several meters into the weathered bedrock (second panel Figure 16). The local water table responds during this first storm despite the lack of deep wetting front penetration; in fact, it responds when the depth of wetting may not have fully wetted up the saprolite. Diffusive transport through the argillite is likely very slow, and probably cannot be sufficient to explain either the relatively rapid deep wetting of the weathered bedrock zone or the rapid delivery to the groundwater.

This rapid, deep response suggests that fracture flow predominates, but the mechanism by which this occurs is not observed in our data. *Heppner et al., [2007],* in their investigation of recharge processes through the vadose zone in weathered fractured sedimentary bedrock, summarized relevant fracture studies for humid environments.

They point out that along fractures, kinematic waves, pressure waves, and air entrapment may matter. *Nimmo, [2010]* offers a recent review of fracture and matrix flow theory and observation in the unsaturated zone, and proposes a specific model to predict, among other things, a rapid deep-water-table response to rain storms (using as an example the results of the [*Heppner et al., 2007*] observations). He draws the distinction between diffuse flow in the matrix and "source-responsive" flow along preferential pathways (including fractures). He proposes this term to highlight that flow can respond "sensitively" to changing rainfall conditions and proposes a model that treats it as a free-surface film of laminar flow. The matrix blocks do not need to be saturated for this to occur, [e.g., *Duke et al., 2007*]. The effective porosity is likely very low, such that relatively small additions of water can cause relatively high groundwater rises.

We propose that the saprolite, which lies between the fracture-free soil and the highly fractured deeper weathered bedrock, may play an important role in feeding the fracture flow system. It is a transitional material, having elevated moisture holding capacity compared to the deeper fractured rock, but retaining a relict fracture system that may serve as pathways to the deeper fracture system that provide rapid delivery to the groundwater. Though the data do not provide a quantitative measure of moisture, the ERSAS data do suggest that the saprolite does not drain rapidly between storm events. It may be, then, that relatively small increases in moisture in the saprolite cause accelerated drainage to fractured networks that drain into the deeper weathered bedrock. It may be that lack of soil structure in the fines produced in the saprolite weathering causes it to be less well drained than the soil. The saprolite, too, may serve as a primary source of rock moisture for the forest.

In the third panel of Figure 16, we show a winter-time hydrologic event, emphasizing that the water table is rising and falling despite the lack of detectable change in water content in the lower portions of the unsaturated zone. Flow of the groundwater is interpreted to be parallel to the fresh bedrock boundary, which acts as a nearly no-flow boundary. At this stage, groundwater dynamics are controlled by lateral as well as vertical flow. Not shown, but very evident in the data, is the widely varying response magnitude at individual wells to a given storm. There is not a simple uniformly rising and falling perched groundwater table on this site. Heterogeneity of groundwater response has

been emphasized by others in hillslope studies [e.g., *Montgomery et al., 1997*; *Ebel et al., 2008*; *Heppner et al., 2007*]. Given the large amount of recharge that must occur to match stream runoff (over 1400 mm), there must be significant net flow through the fracture network. The dynamics may still be influenced by kinematic and pressure waves.

From a study of solute transfer through the unsaturated zone and shallow groundwater in weathered granite at the upslope portion of a hill, [*Legout et al., 2007*] proposed distinguishing a chronically unsaturated zone from a zone subject to water table fluctuations and from a lower permanently saturated zone. They argued that in each zone, the interplay of rapid mobile water, inferred to be travelling through larger pores, and slower moving water differed. [*Van der Hoven et al., 2005*] proposed that rapid fluxes of water recharge along fractures in a saprolite developed on shale and limestone bedrock leads to significant temporal variation in the underlying groundwater. A variation in the interplay between matrix water and fracture water in the three such zones in our study site (soil, saprolite and weathered bedrock) may occur and influence the chemical evolution of water.

The shallow TDR measurements (not embedded in silica flour) and neutron probe surveys reveal a summer soil- and rock-moisture loss of about 100 and 115 mm respectively. This is a direct measure of how much moisture change occurred, not how much is stored in the rock, and it may well be that the deeper weathered bedrock zone remains close to saturation all year long. As other studies have proposed, the abundance of rock moisture provides a crucial water source beyond soil moisture for seasonally dry environments [e.g., *Schwinning, 2010*; *Zwieniecki and Newton, 1996*]. It is worth noting, in particular, that in fractured metasedimentary rocks in southwestern Oregon, [*Zwieniecki and Newton, 1996*] estimated that there was 172 mm of available water holding capacity in the first 2.8 m thick layer of rock—of which young Douglas fir (*Pseudotsuga*) and ponderosa pine (*Pinus ponderosa*) used up to 40%, whereas madrone (*Arbutus*) and Manzanita (*Arctostaphylos*) used 70 to 96%. Here, we show a deeper rock-moisture zone, one that recovers from seasonal drying in the first rains of the fall, and is probably tapped by vegetation and replenished with rain throughout the wet season, at least by the Douglas Fir on our north-facing slope. We also see systematic

variation in rock-moisture dynamics from the near the channel to close to the hilltop. The structure of the weathered bedrock zone and the exposure of the hillslope appear to be important to rock-moisture availability and use. Our study site is north-facing: we hypothesize that more active wet season use of rock moisture by hardwoods occurs on south-facing slopes.

5.4 Seasonal storage and runoff

Recently [Sayama et al., 2011] used rainfall-runoff data from two watersheds ~130 km north of our study site (underlain by similar bedrock), calculations of actual evapotranspiration (and ignoring interception) to suggest that in their seasonally dry landscape, about 200-500 mm of precipitation must accrue before "storm runoff "is generated. They use field observations in the Oregon Coast Range in sedimentary rocks (e.g. Anderson et al, 1997; Anderson and Dietrich, 2001, and Dietrich and Montgomery , 2002) to infer that this storage occurs at depths below the soil and speculate about how hillslope gradient may matter. Our direct measurements show that the infiltrating rainfall goes into storage as moisture in the soil, moisture in the weathered bedrock, and in the groundwater perched on fresh bedrock. Storage effects are dramatic. The first significant rains recharge the moisture in the soil and weathered bedrock, with some water rapidly reaching the perched groundwater via fractures. Correspondingly, Elder Creek (to which our site drains) responds to these rains, but the magnitude is small (Figure 5). In subsequent rain storms, the soil moisture rises and falls but remains elevated, and the rock moisture remains relatively constant. Progressively, the water table rises (rates differing across the hillslope) and its elevated position is sustained by repeated pulses of rain. The soil and rock moisture reach a quasi-steady value first, followed the elevated groundwater. The system reaches this state after about 400 mm of cumulative total rain (similar to what Sayama et al report). Storm runoff occurs via perched groundwater flow and rapid response is most likely due to rapid transmission along fractures, first vertically through the unsaturated zone, and then laterally through the groundwater. It is the rise of this perched groundwater system, fed by rapid delivery along fractures after soil and rock moisture buildup has occurred, that leads to significant storm runoff.

6. Conclusions

The development of a weathered bedrock zone, one that thickens upslope from the channel towards the hillslope divide, creates a deep, hydrologically active domain through which seasonal rainfall rapidly penetrates and recharges a groundwater table perched on underlying fresh bedrock. Within the weathered bedrock zone, the intensity of fracturing and the degree of weathering decrease with depth. It is capped by a stony, porous, fracture free soil about 50 cm thick. All runoff occurs through the perched, groundwater system. Here, we distinguish between soil moisture and rock moisture, the latter referring to both exchangeable matrix water and fracture water in the unsaturated weathered bedrock. *Rock moisture* is not a term of use, but given the growing recognition that such moisture is seasonally dynamic and represents a significant moisture resource to vegetation, it warrants separate quantification.

In the Mediterranean climate of our field site, after up to 6 months of no rain, the soil moisture is reduced to about 5%, and the weathered bedrock moisture is at a minimum. The first large storms of the fall cause water to be injected as much as 6 m below the surface, well below the soil layer. In most cases, however, the groundwater level (about 5 to 19 m below the surface at the start of winter rains) noted at seven wells rose in a few hours, before the advancing increased moisture front had reached just 1 m into the ground. Throughout the winter, groundwater rose and fell in response to pulses of rain, but typically the lower portion of the unsaturated zone showed no temporal variation in rock moisture. Shallow weathered bedrock, sufficiently altered to be called a saprolite, seasonally gained and lost rock moisture, but showed little variation in moisture content during the winter rainy period, and dried much more slowly than the overlying soil. Soil moisture rose and fell with each storm pulse. Hence, it appears that the saprolite may be a near-surface layer of elevated rock moisture that may influence water delivery to depth and water availability to vegetation, especially in the summer. In response to the succession of winter rains, local groundwater response differed greatly among the wells and through the season.

The first fall rains quickly restored diminished moisture levels in the soil and rock. The summer (no rain) depletion led to comparable losses of moisture in the soil and

weathered bedrock (a total of about 200 mm), with detectable rock-moisture loss as much as 11 m below the surface. As a consequence, the rock-moisture zone may roughly double the water available to vegetation, with some soil-moisture loss to evaporation and, perhaps, some rock-moisture loss due to deep drainage. This is an essentially unmapped moisture reservoir under the hillslope.

We present a conceptual model to explain these dynamics, one suggesting that the rapid-delivery mechanism of unsaturated flow, and thus recharge, to the water table is through a vertically varying fracture network bounded by low-conductivity matrix bedrock. The near-surface saprolite may play an important role in creating elevated moisture conditions sufficient to cause rapid drainage to the fracture system with incoming rains. Various models have been proposed for how a coupled matrix and fracture-flow system works in the unsaturated zone. Our observations offer some constraints, but one challenge here is the extraordinary heterogeneity of response at different locations across our hillside. Soil- and rock-moisture dynamics also differ systematically up the hillslope—owing, perhaps to both material and environmental demand differences on this north-facing hilllslope. Further experimental investigations, including the simulation of rainfall and the tracing of water chemistry, should further constrain flow mechanisms and controls on soil- and rock-moisture dynamics.

Acknowledgements

This work was supported by Laboratory Directed Research and Development (LDRD) funding from Berkeley Lab, provided by the Director, Office of Science, of the U.S. Department of Energy under Contract No. DE-AC02-05CH11231, the Keck Foundation, and the National Center for Earth-surface Dynamics. The topographic map was derived from data provided to Mary Power (University of California, Berkeley) by the National Center for Airborne Laser Mapping. Daniella Rempe is supported in part by the Department of Energy Office of Science Graduate Fellowship Program (DOE SCGF), made possible in part by the American Recovery and Reinvestment Act of 2009, administered by ORISE-ORAU under contract no. DE-AC05-06OR23100. Reviews by Dan Hawkes, John Nimmo and two anonymous reviewer are gratefully acknowledged.

References

Anderson, S. P., and W. E. Dietrich (2001), Chemical weathering and runoff chemistry in a steep headwater catchment, *Hydrological Processes*, *15*(10), 1791-1815.

Anderson, S. P., W. E. Dietrich, D. R. Montgomery, R. Torres, M. E. Conrad, and K. Loague (1997), Subsurface flow paths in a steep, unchanneled catchment, *Water Resources Research*, *33*(12), 2637-2653.

Banks, E. W., C. T. Simmons, A. J. Love, R. Cranswick, A. D. Werner, E. A. Bestland, M. Wood, and T. Wilson (2009), Fractured bedrock and saprolite hydrogeologic controls on groundwater/surface-water interaction: a conceptual model (Australia), *Hydrogeology Journal*, *17*(8), 1969-1989.

Bureau, U. S. W. (1968), Climatological Data, California, *US Dept. Commerce*, *72*, 1-454.

Burns, D. A. et al. (2003), The geochemical evolution of riparian ground water in a forested piedmont catchment, *Ground Water*, *41*(7), 913-925.

Dalton, F. (1992), Development of time-domain reflectometry for measuring soil water content and bulk soil electrical conductivity, *SSSA special publication series*.

Duke, C. L., R. C. Roback, P. W. Reimus, R. S. Bowman, T. L. McLing, K. E. Baker, and L. C. Hull (2007), Elucidation of flow and transport processes in a variably saturated system of interlayered sediment and fractured rock using tracer tests, *Vadose Zone Journal*, *6*(4), 855-867.

Dunne, T. (1978), Field studies of hillslope flow processes, *Hillslope hydrology*, *227*, 293.

Ebel, B. A., K. Loague, D. R. Montgomery, and W. E. Dietrich (2008), Physics-based continuous simulation of long-term near-surface hydrologic response for the Coos Bay experimental catchment, *Water Resources Research*, *44*(7), W07417.

Faybishenko, B., P.A. Witherspoon, and J. Gale (2005), *Dynamics of fluids and transport in fractured rock*, Amer Geophysical Union.

Freer, J., J. McDonnell, K. J. Beven, D. Brammer, D. Burns, R. Hooper, and C. Kendal (1997), Topographic controls on subsurface stormflow at the hillslope scale for two hydrologically distinct small catchments., *Hydrological Processes*, *11*(9), 1347-1352.

Fuller, T. K., L. A. Perg, J. K. Willenbring, and K. Lepper (2009), Field evidence for climate-driven changes in sediment supply leading to strath terrace formation, *Geology*, *37*(5), 467-470.

Gburek, W., and J. Urban (1990), The Shallow Weathered Fracture Layer in the Near-Stream Zone, *Ground Water*, *28*(6), 875-883.

Gburek, W. J., and G. J. Folmar (1999), A groundwater recharge field study: site characterization and initial results, *Hydrological processes*, *13*(17), 2813-2831.

Ghezzehei, T. A. (2008), Errors in determination of soil water content using time-domain reflectometry caused by soil compaction around wave guides,

Heppner, C. S., J. R. Nimmo, G. J. Folmar, W. J. Gburek, and D. W. Risser (2007), Multiple-methods investigation of recharge at a humid-region fractured rock site, Pennsylvania, USA, *Hydrogeology Journal*, *15*(5), 915-927.

Van der Hoven, S. J., D. Kip Solomon, and G. R. Moline (2005), Natural spatial and temporal variations in groundwater chemistry in fractured, sedimentary rocks: scale and implications for solute transport, *Applied geochemistry*, *20*(5), 861-873.

Ireson, A., S. Mathias, H. Wheater, A. Butler, and J. Finch (2009), A model for flow in the chalk unsaturated zone incorporating progressive weathering, *Journal of Hydrology*, *365*(3-4), 244-260.

Kampf, S. K., and S. J. Burges (2007), A framework for classifying and comparing distributed hillslope and catchment hydrologic models, *Water Resour. Res*, *43*, W05423.
Katsura, S, K. Kosugi,, T., Mizutani, S, Okunaka, and T. Mizuyama,(2008) Effects of bedrock groundwater on spatial and temporal variations in soil mantle groundwater in a steep granitic headwater catchment, *Water Resour. Res*, *44*, W01407,

Kim, H., J. Bishop, T. Wood, I. Fung (In Press), Autonomous water sampling for a long-term monitoring of trace metals in remote environments, *Environmental Science & Technology*.

Kim, H., J. Bishop, T. Wood, I. Fung, and M. Fong (2011), Automation of high-frequency sampling of environmental waters for reactive species, *AGU Fall Meeting Abstracts*, *1*, 1160.

Kosugi, K,, S. Katsura, T. Mizuyama,,S. Okunaka, and T. Mizutani, T, (2008) Anomalous behavior of soil mantle groundwater demonstrates the major effects of bedrock groundwater on surface hydrological processes *Water Resour. Res*, *44*, W09430,

Legout, C., J. Molenat, L. Aquilina, C. Gascuel-Odoux, M. Faucheux, Y. Fauvel, and T. Bariac (2007), Solute transfer in the unsaturated zone-groundwater continuum of a headwater catchment, *Journal of Hydrology*, *332*(3), 427-441.

Link, P., I. Fung, and K. Simonin (2011), Heterogeneity in Light and Water Availability Drives Sap Flow Patterns in Steep Terrain, *AGU Fall Meeting Abstracts*, *1*, 08.

Long, I., and B. French (1967), Measurement of soil moisture in the field by neutron moderation, *Journal of Soil Science*, *18*(1), 149-166.

McDonnell, J. J. (1990), A rationale for old water discharge through macropores in a steep, humid catchment, *Water Resour. Res*, *26*(11), 2821-2832.

McGlynn, B. L., J. J. McDonnel, and D. D. Brammer (2002), A review of the evolving perceptual model of hillslope flowpaths at the Maimai catchments, New Zealand, *Journal of Hydrology*, *257*(1), 1-26.

McKay, L. D., S. G. Driese, K. H. Smith, and M. J. Vepraskas (2005), Hydrogeology and pedology of saprolite formed from sedimentary rock, eastern Tennessee, USA, *Geoderma*, *126*(1-2), 27-45.

McLaughlin, R. J., S. Ellen, M. Blake Jr, A. S. Jayko, W. Irwin, K. Aalto, G. Carver, and S. Clarke Jr (2000), Geology of the Cape Mendocino, Eureka, Garberville, and Southwestern Part of the Hayfork 30 x 60 minute Quadrangles and adjacent offshore area, Northern California, *US Geological Survey Miscellaneous Field Studies MF-2336, Washington, DC*.

Miralles, D. G., J. H. Gash, T. R. H. Holmes, R. A. M. de Jeu, and A. Dolman (2010), Global canopy interception from satellite observations, *J. Geophys. Res.-Atmos*, *115*, D16122.

Montgomery, D. R., and W. E. Dietrich (1994), A physically based model for the topographic control on shallow landsliding, *Water resources research*, *30*(4), 1153-i171.

Montgomery, D. R. K. Schmidt,, W. E. Dietrich, and J. McKean (2009), Instrumental record of debris flow initiation during natural rainfall:Implications for modeling slope stability, *Jour. Geophy. Res.*, 114 F01031

Montgomery D. R. and W. E. Dietrich (2002), Runoff generation in a steep, soil-mantled landscape, *Water Resources Research*, *38*(9), 1168.

Montgomery, D. R., W. E. Dietrich, R. Torres, S. Prestrud Anderson, J. T. Heffner, and K. Loague (1997), Hydrologic response of a steep, unchanneled valley to natural and applied rainfall, *Water Resources Research*, *33*(1), 91-109.

Nimmo, J. R. (2010), Theory for source-responsive and free-surface film modeling of unsaturated flow, *Vadose Zone Journal*, *9*(2), 295-306.

Oshun, J., R. Salve, D. Rempe, W. Dietrich, and I. Fung (2010), Fractured Bedrock Storm Flow: a New Pathway for Runoff Generation, *AGU Fall Meeting Abstracts*, *1*, 0691.

Pack, R., D. Tarboton, and C. Goodwin (1998), The SINMAP approach to terrain stability mapping, *8th congress of the international association of engineering geology, Vancouver, British Columbia, Canada*, 21-25.

Reid, L. M., and J. Lewis (2009), Rates, timing, and mechanisms of rainfall interception loss in a coastal redwood forest, *Journal of Hydrology*, *375*(3), 459-470.

Rempe, D., J. Oshun, W. Dietrich, R. Salve, and I. Fung (2010), Controls on the weathering front depth on hillslopes underlain by mudstones and sandstones, *AGU Fall Meeting Abstracts*, *1*, 05.

Reynolds, J. M. (2011), *An introduction to applied and environmental geophysics*, Wiley.

Rosso, R., M. C. Rulli, and G. Vannucchi (2006), A physically based model for the hydrologic control on shallow landsliding, *Water Resour. Res*, *42*(6), W06410.

Sakaki, T., and H. Rajaram (2006), Performance of different types of time domain reflectometry probes for water content measurement in partially saturated rocks, *Water resources research*, *42*(7), 7404.

Salve, R. (2011), A sensor array system for profiling moisture in unsaturated rock and soil, *Hydrological Processes*.

Sayama, T., J.J. McDonnell,2 A. Dhakal, and K/ Sullivan, (2011) How much water can a watershed store? Hydrol. Process. 25, 3899–3908 .

Schwinning, S. (2010), The ecohydrology of roots in rocks, *Ecohydrology*, *3*(2), 238-245.

Shand, P., D. Darbyshire, D. Gooddy, and A. H Haria (2007), 87Sr86 Sr as an indicator of flowpaths and weathering rates in the Plynlimon experimental catchments, Wales, UK, *Chemical geology*, *236*(3), 247-265.

Sidle, R. C., Y. Tsuboyama, S. Noguchi, I. Hosoda, M. Fujieda, and T. Shimizu (2000), Stormflow generation in steep forested headwaters: a linked hydrogeomorphic paradigm, *Hydrological Processes*, *14*(3), 369-385.

Simonin, K., P. Link, J. Oshun, D. Rempe, T. Dawson, W. Dietrich, and I. Fung (2010), Plant d-excess: a new concept and tool for exploring plant-soil-atmospheric water cycling, *AGU Fall Meeting Abstracts.*

Topp, G., J. Davis, A. P. Annan, and others (1980), Electromagnetic determination of soil water content: Measurements in coaxial transmission lines, *Water Resour. Res*, *16*(3), 574-582.

Tromp-van Meerveld, H. J., N. E. Peters and J. J. McDonnell (2007) Effect of bedrock permeability on subsurface stormflow and the water balance of a trenched hillslope at the Panola Mountain Research Watershed, Georgia, USA, *Hydrological Processes* 21: 750-769.

Wilson, C., and W. Dietrich (1987), The contribution of bedrock groundwater flow to storm runoff and high pore pressure development in hollows, *IN: Erosion and Sedimentation in the Pacific Rim. IAHS Publication,* (165).

Wilson, C., W. Dietrich, and T. Narasimhan (1989), Predicting high pore pressures and saturation overland flow in unchannelled hillslope valleys, *Hydrology and Water Resources Symposium 1989: Comparisons in Austral Hydrology; Preprints of Papers,* 392.

Zwieniecki, M. A., and M. Newton (1996), Seasonal pattern of water depletion from soil-rock profiles in a Mediterranean climate in southwestern Oregon, *Canadian Journal of Forest Research, 26*(8), 1346-1352.

Figure Captions

Figure 1. Rivendell study site showing contours (1m intervals) derived from airborne laser swath mapping data collected by the National Center for Airborne Laser Mapping and the location of wells and instruments used for this study. Patterned area is shows the spatial extent of a sandstone interbed that has little to no soil cover. The labels "TDR" refer to time domain reflectometry (S- installed vertically, T horizontally), ERP labels the location of the ERSAS resistivity probes set in vertical profiles. The "stream gauge" records Elder Creek water level. Inset shows the location of the Rivendell study site relative to Elder Creek and the South Fork Eel River into which Elder Creek drains.

Figure 2. Profile of the site showing the soil layer mantling a tapered weathered, fractured argillite zone over fresh bedrock. The three hydrologic states of the weathered rock zone are shown: unsaturated throughout the year (white), saturated throughout the year (dark gray), and subject to seasonal saturation (light gray).

Figure 3. (A) Sketch showing vertical profile of ERSAS and TDR installations Note the boreholes used to locate the probes extended to a vertical distance of ~2 m from the surface. Each TDR probe was 0.30 m long and the ERSAS sensors were spaced 0.10 m apart. (B) ERSAS sensor design showing two electrical leads located between pieces of filter paper and wire mesh, and (C) Location of sensors along a support stem. The length of the stem and the spacing between sensors can be adjusted for specific applications.

Figure 4. Sketch defining the parameters (i) lag to peak and (ii) transit time used to analyze the soil and fractured rock response to individual storm events. Data used in the figure is from a storm event at the study site in early February, 2012.

Figure 5. Example of temporal pattern of data collected at Rivendell for the period of two years beginning in September 2008. (A) Rainfall distribution at Rivendell. Vertical lines indicate cumulative rainfall measured for individual events. Also included is the cumulative rainfall for the duration of the season. (B) Soil moisture content measured at 0-0.5 m from surface and (C) Stage at Elder Creek and location of water table relative to the ground surface at Wells 6 & 7.

Figure 6. Detection of early season wetting in soil moisture profiles in response to the first September and October storm. Data from all (A) ERSAS and (B) TDR profiles are shown together and staggered for visibility. Columns, from left to right, are associated with storms that occurred on September 13, 2009, October 12, 2009, September 19, 2010, and October 22, 2010. Probes located in soil, indicated by square symbols, are typically located at depths shallower than 50 cm however wetting is detected at depths up to 0.9 m for September storms and there is greater than 2 m penetration in October.

Figure 7. Magnitude and duration of the first major storms for 2008. 2009 and 2010. Colored dots indicate the first seasonal rise in the water table detected in wells along the hillslope in response to these early season rain events.

Figure 8. Depth profile of detection of moisture increase by the ERSAS and TDR probes in response to seasonal cumulative rainfall (water years 2008 and 2009).Along the 'x' axis in each

figure the tick marks with labels (i.e.1, 2,3, & 10) indicate the first rise in water table levels as detected in wells closest to each ERSAS/TDR nest.

Figure 9. Comparison of the response between selected ERSAS sensors and neighboring SM200 probes (installed at about 30 cm depth) in response to precipitation during the (A) 2008-2009 and (B) 2009-2010 water years. The precipitation data, recorded at 15 minute intervals, is normalized by the maximum 15 minute rainfall rate of the year. The sensor response is normalized by the maximum sensor response for the entire monitoring period.

Figure 10. ERSAS response for three representative profiles at (A) Level 1, (B) Level 2 and (C) Level 3, from October 1 2009 to October 1 2010.

Figure 11. Seasonal dynamics in soil moisture at during 2008-2009 as recorded by the TDR- T series probes (right) and ERSAS (left).

Figure 12. TDR-T (horizontal) series measurements of soil moisture content at level 2. Relative precipitation is shown in black for reference. Dotted lines mark the summer dry season.

Figure 13. Neutron probe measurements made along the length of 6 of the seven monitored wells. Along the length of each well neutron counts were measured at 0.30 m intervals. Shown on each plot are the difference in neutron counts between measurements made in October 28, 2008. Gray bars indicate the location of the water table at the time of measurement.

Figure 14. (A) Groundwater and (B) rock-moisture response at well 3 to two storms that dropped a total of 260 mm of rain between October 10 and November 5, 2010.

Figure 15. Change in rock-moisture content detected across the hillslope between October 10 and November 5, 2010. Two storms brought a total of 260 mm between the measurement dates. Soil depths are marked by gray bars in Wells 1-3. Wells 5, 6, and 7 are located on a dirt road lacking soil.

Figure 16. Conceptual model showing possible mechanisms to explain the rock-moisture and groundwater dynamics observed in the weathered bedrock zone.

Authors	Study Site	Bedrock type	Bedrock flow (%)
Katsuyama et al. (2004)	Kiryu Watershed , Central Japan	Granite	45[a]
Kosugi et al., 2006	Kiryu Watershed , Central Japan	Granite	35-55[a]
Tromp van Meerveld et al. (2007)	Panola Watershed, Georgia, USA	Granite	14-21[b]
Uchida et al.(2003)	Fudoji Catchment, Japan	Granite	50-95[b]
Kosugi et al., (2006)	Kiryu Watershed , Central Japan	Granite	65-71[b]
Anderson and Dietrich (2001)	Oregon, USA	Sandstone	93[b]
		[a] Rainfall infiltrating into bedrock, field study	
		[b]Bedrock contribution to stream flow, field study	

Table 1. Amount of recharge/discharge associated with bedrock flow determined from recent field investigations.

Season	Duration of wet season (days)	Total Precipitation (mm)	Number of storm events	Avgerage Precipitation per event (mm)	Period between storm events (days)	
					Avg	Max
2007-08	237	1338	43	31	5	31
2008-09	257	1479	51	29	4	28
2009-10	239	1883	63	30	3	17
2010-11	295	2106	81	26	3	32

Table 2. Season rainfall characteristics for the four year monitoring period.

Storm Start	Storm Centroid	Storm Peak	Storm Cumulative Rainfall (mm)	Storm Duration (hours)	Average Intensity (mm/hour)	Peak 15 Minute Rainfall Intensity (mm/hour)
10/3/2008 8:30	10/3/2008 17:16	10/3/2008 17:02	96	28	3	13
10/12/2009 7:52	10/13/2009 13:40	10/13/2009 12:57	134	43	3	24
10/22/2010 23:02	10/23/2010 15:21	10/23/2010 23:02	220	41	5	29

Table 3. Details for the first major storms for three of the four years of monitoring. The rainfall data for the early part of the 2007 water-year was not collected.

Year	Well	Time to Response (hours)	Water Table Depth (m)	Velocity of Response (cm/hr)	Cumulative Rainfall to Response (mm)	Magnitude of Peak Well Response (m)	Lag to peak (hours)	Magnitude of Response (m)
2008	1	16	4.56	29	75	4.17	17.7	0.39
2008	2	9	12.13	143	42	11.67	12.2	0.46
2008	3	3	9.77	391	9	9.47	0.2	0.30
2008	5							
2008	6							
2008	7	3	15.90	530	11	15.81	-17.3	0.09
2008	10	8	18.13	227	37	-18.00	-17.3	0.13
2009	1	18	4.54	26	2	3.84	26.8	0.70
2009	2	30	12.10	41	63	11.42	24.8	0.68
2009	3	21	9.83	47	18	9.14	0.8	0.69
2009	5							
2009	6	53	11.13	21	129	10.78	120.8	0.35
2009	7	14	14.88	105	1			
2009	10	28	17.65	64	45	17.35	1.3	0.30
2010	1	27	4.27	16	77	2.93	20.1	1.34
2010	2							
2010	3	33	10.05	30	184	3.95	8.6	6.10
2010	5	62	21.55	35	227			
2010	6	36	11.01	31	212	10.54	53.6	0.47
2010	7	23	14.02	61	41	13.52	19.1	0.50
2010	10	22	17.26	79	34	16.71	18.1	0.55

Table 4. Groundwater response to first major storm of the season as detected in the seven monitoring wells located across the hillslope. The time to response (column 3) and lag to peak (column 8) are defined in Figure 4. Here velocity of response (Column 6) is calculated as the depth to water table divided by the time to response.

	2008-2009	2009-2010	2010-2011
Precipitation (mm)	1490	1910	2090
Runoff (mm)	782	1330	1480
Interception (mm)	194	248	271
Evapotranspiration (mm)	514	332	339
Runoff ratio	0.53	0.70	0.71
ET/Precipitation	0.35	0.17	0.16
Summer moisture change in soil (mm)	111	56	
Summer moisture change in weathered bedrock (mm)	115	115	
Total summer moisture change (mm)	226	171	

Table 5. Annual water balance for Elder Creek. Note because of sensor malfunctions during the summer of 2011 the water balance could not be completed for that water-year.

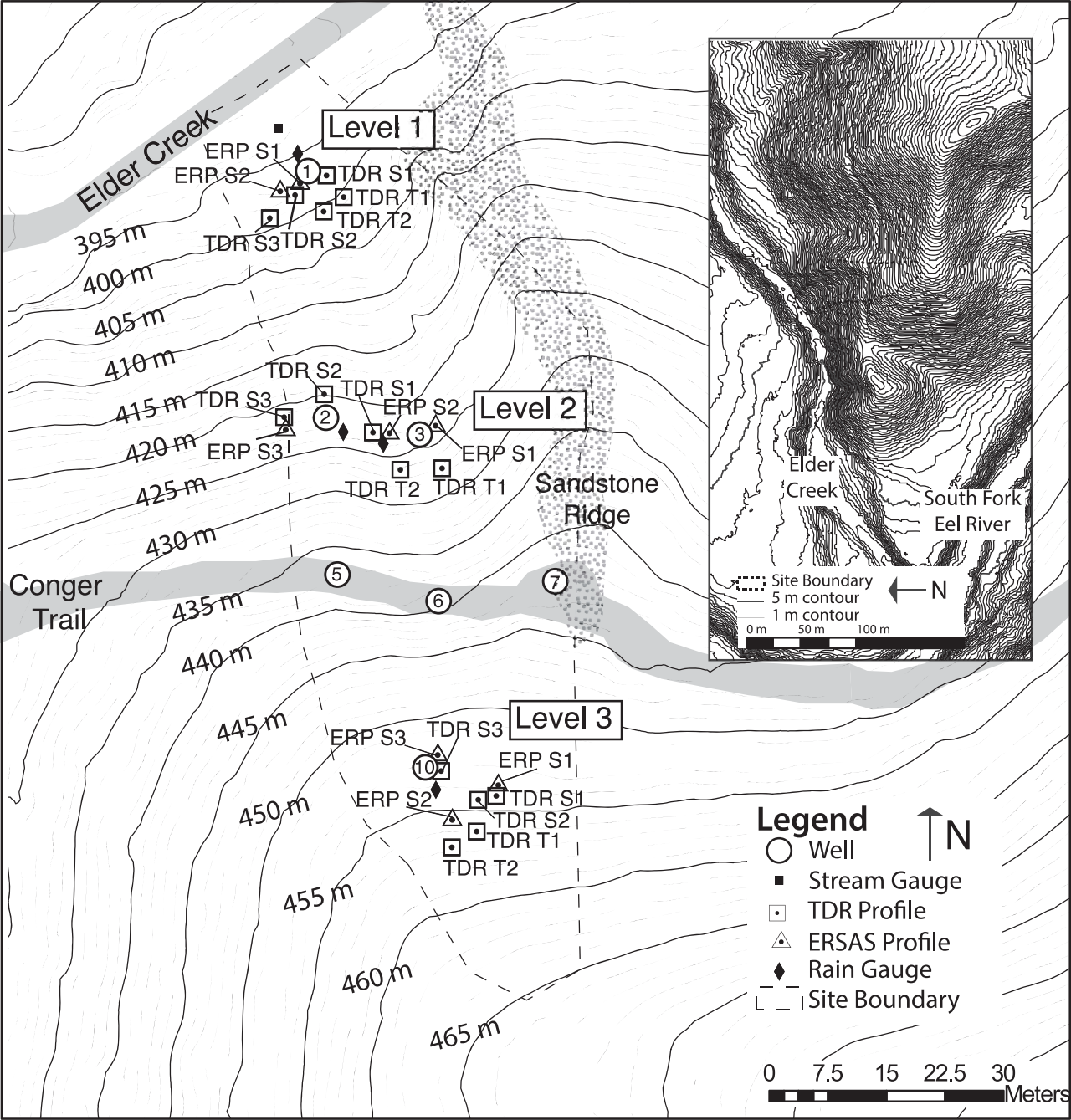
Elder Creek
Level 1
ERP S1
ERP S2
TDR S1
TDR T1
TDR T2
TDR S3
TDR S2
395 m
400 m
405 m
410 m
415 m
420 m
425 m
430 m
435 m
440 m
445 m
450 m
455 m
460 m
465 m
Level 2
TDR S2
TDR S1
TDR S3
ERP S2
ERP S3
ERP S1
TDR T2
TDR T1
Sandstone Ridge
Conger Trail
Level 3
ERP S3
TDR S3
ERP S1
ERP S2
TDR S1
TDR S2
TDR T1
TDR T2
Elder Creek
South Fork Eel River
Site Boundary
5 m contour
1 m contour
N
0 m
50 m
100 m
Legend
Well
Stream Gauge
TDR Profile
ERSAS Profile
Rain Gauge
Site Boundary
N
0
7.5
15
22.5
30
Meters

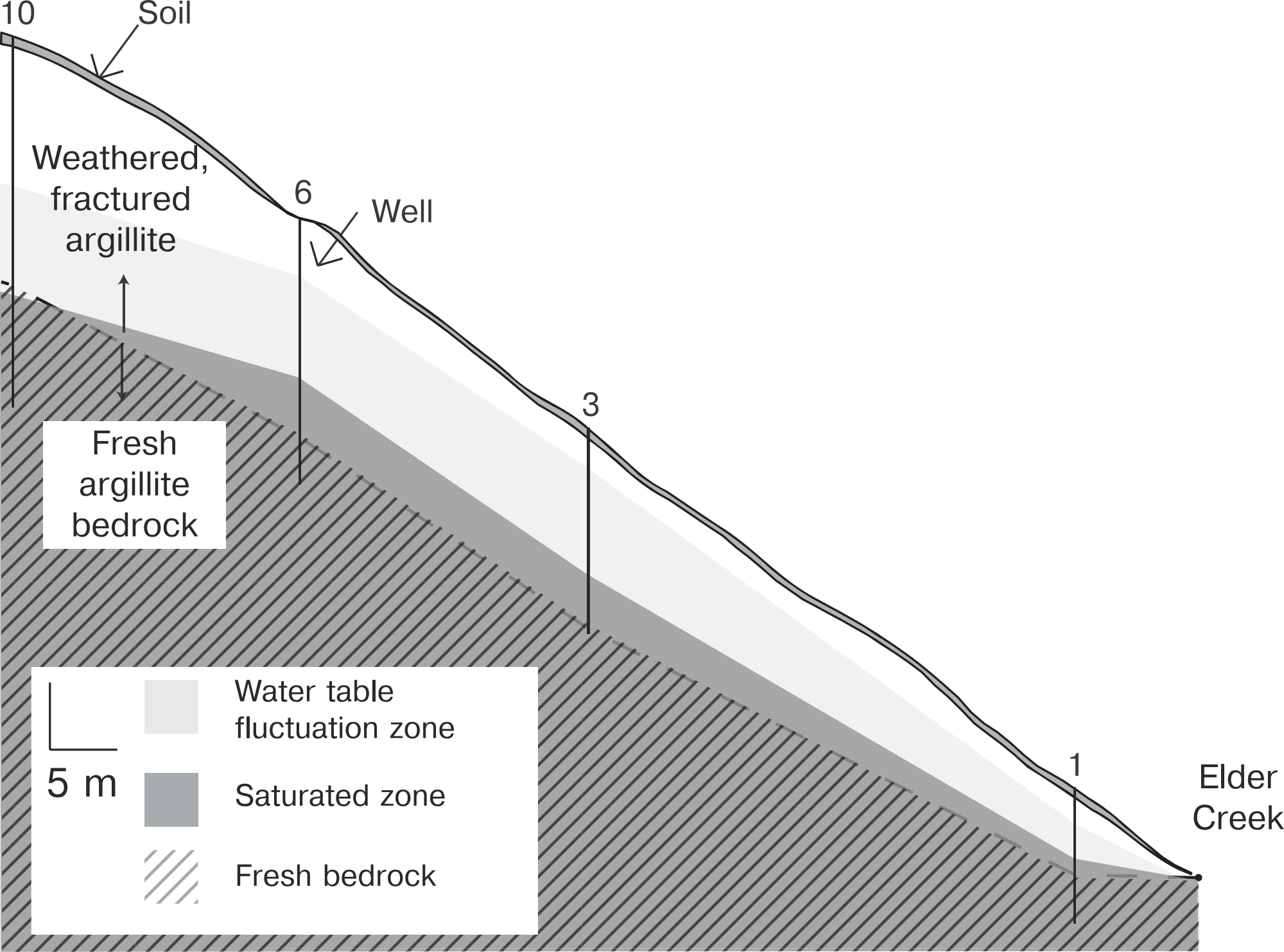
10
Soil
Weathered, fractured argillite
6
Well
3
Fresh argillite bedrock
1
Elder Creek
5 m
Water table fluctuation zone
Saturated zone
Fresh bedrock

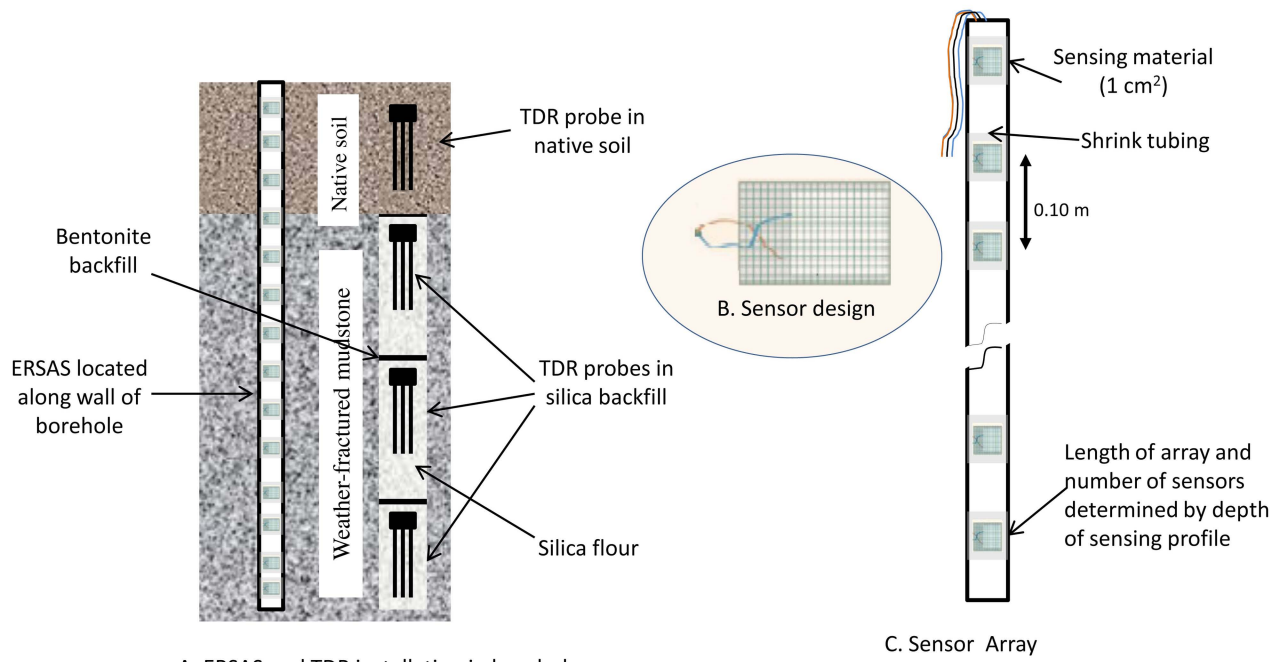
Native soil
TDR probe in native soil
Bentonite backfill
ERSAS located along wall of borehole
Weather-fractured mudstone
TDR probes in silica backfill
Silica flour
A. ERSAS and TDR installation in boreholes
B. Sensor design
Sensing material (1 cm²)
Shrink tubing
0.10 m
Length of array and number of sensors determined by depth of sensing profile
C. Sensor Array

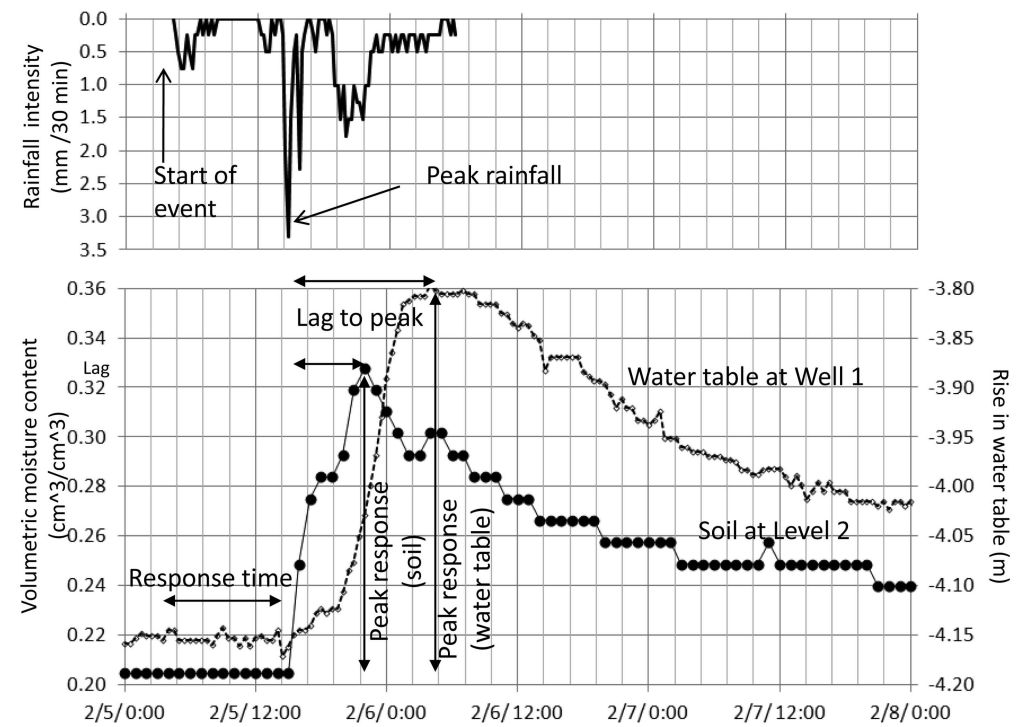
Rainfall intensity (mm /30 min)
0.0
0.5
1.0
1.5
2.0
2.5
3.0
3.5
Start of event
Peak rainfall
Volumetric moisture content (cm^3/cm^3)
0.36
0.34
0.32
0.30
0.28
0.26
0.24
0.22
0.20
Lag
Lag to peak
Response time
Peak response (soil)
Peak response (water table)
Water table at Well 1
Soil at Level 2
Rise in water table (m)
-3.80
-3.85
-3.90
-3.95
-4.00
-4.05
-4.10
-4.15
-4.20
2/5/0:00
2/5/12:00
2/6/0:00
2/6/12:00
2/7/0:00
2/7/12:00
2/8/0:00

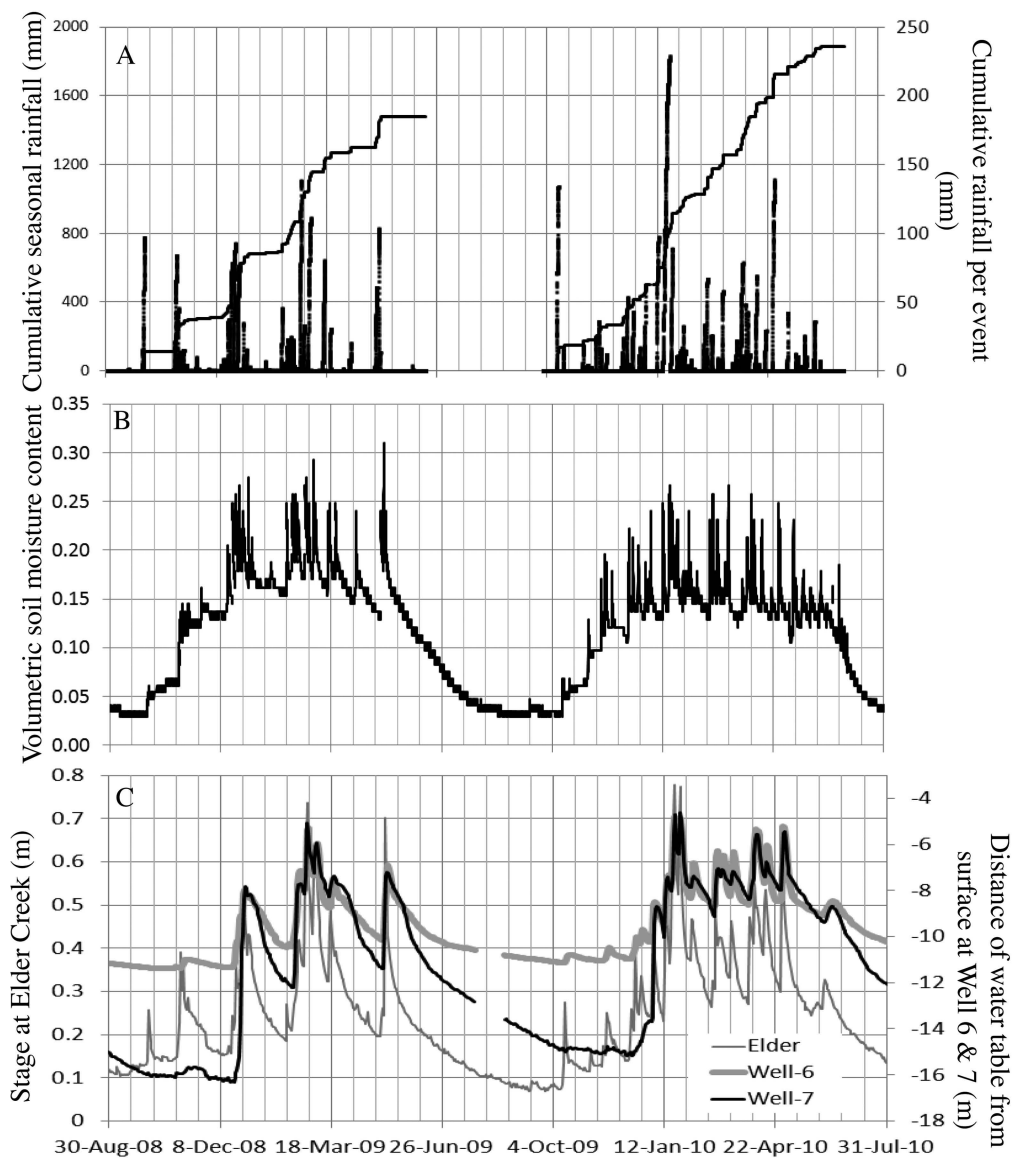
A
B
C
Cumulative seasonal rainfall (mm)
Cumulative rainfall per event (mm)
Volumetric soil moisture content
Stage at Elder Creek (m)
Distance of water table from surface at Well 6 & 7 (m)
Elder
Well-6
Well-7
30-Aug-08
8-Dec-08
18-Mar-09
26-Jun-09
4-Oct-09
12-Jan-10
22-Apr-10
31-Jul-10

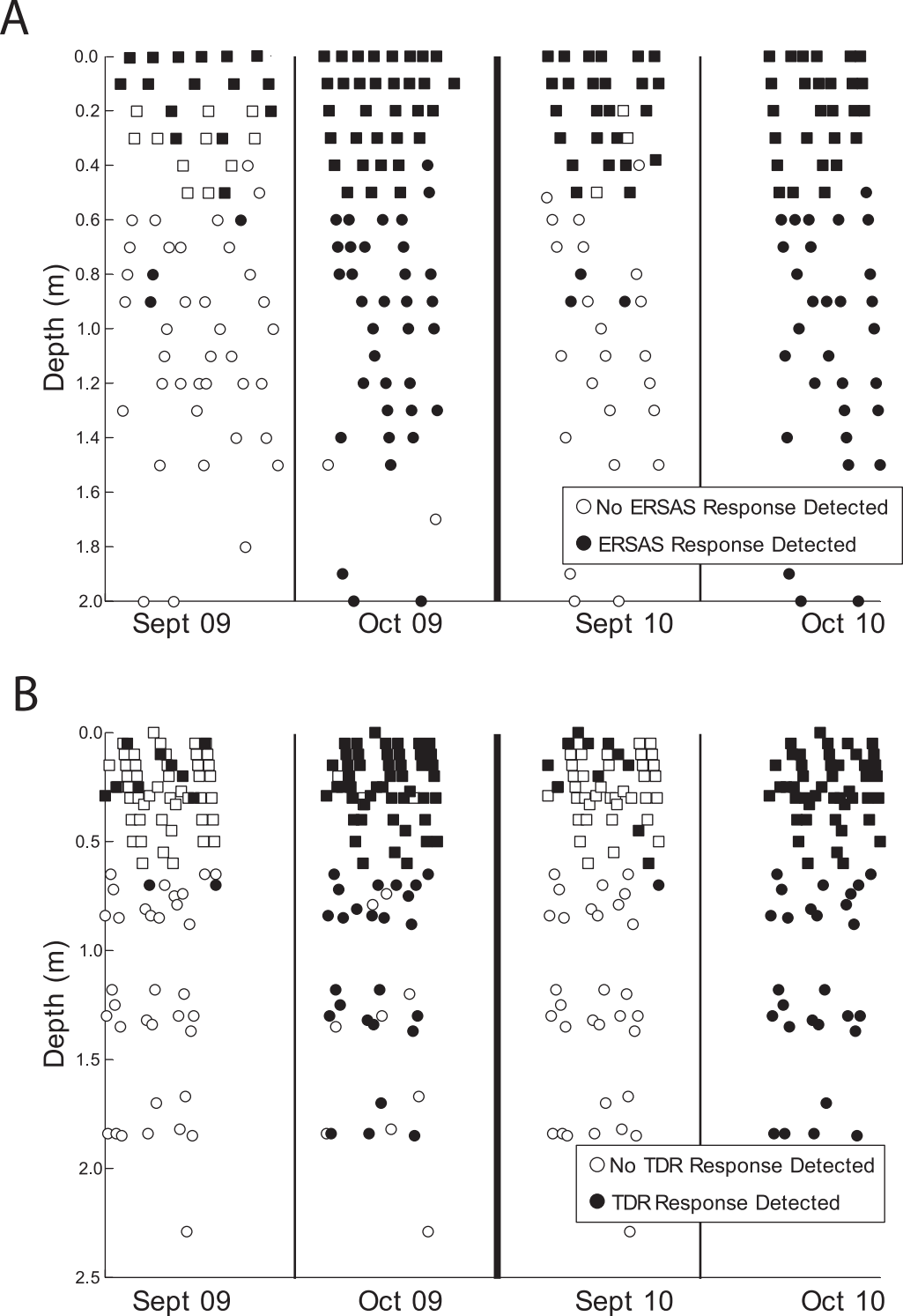
A
Depth (m)
0.0
0.2
0.4
0.6
0.8
1.0
1.2
1.4
1.6
1.8
2.0
No ERSAS Response Detected
ERSAS Response Detected
Sept 09
Oct 09
Sept 10
Oct 10
B
Depth (m)
0.0
0.5
1.0
1.5
2.0
2.5
No TDR Response Detected
TDR Response Detected
Sept 09
Oct 09
Sept 10
Oct 10

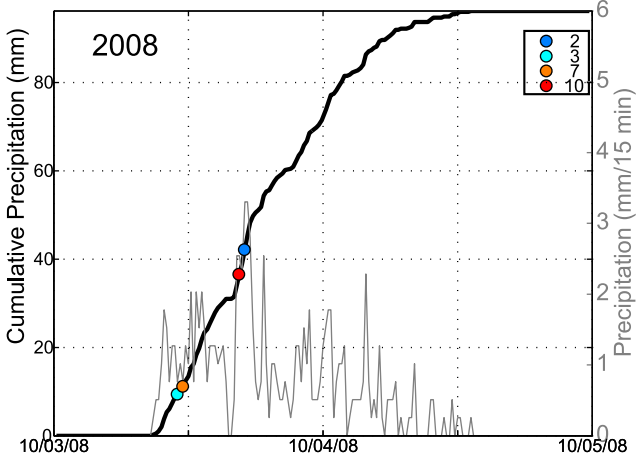
2008
Cumulative Precipitation (mm)
Precipitation (mm/15 min)
2
3
7
10
0
20
40
60
80
1
2
3
4
5
6
10/03/08
10/04/08
10/05/08

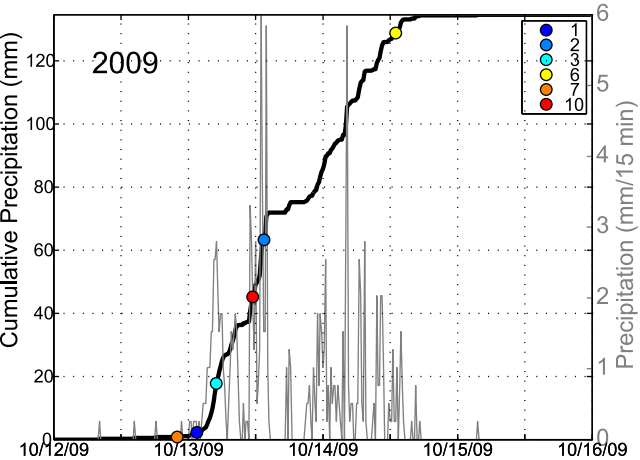
2009
Cumulative Precipitation (mm)
Precipitation (mm/15 min)
1
2
3
6
7
10
0
20
40
60
80
100
120
1
2
3
4
5
6
10/12/09
10/13/09
10/14/09
10/15/09
10/16/09

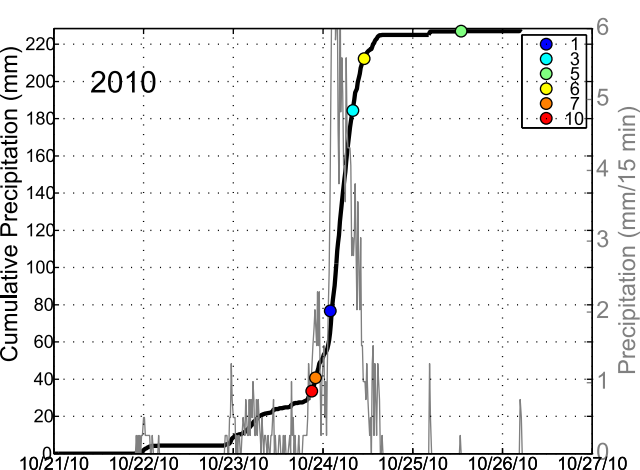
2010
Cumulative Precipitation (mm)
Precipitation (mm/15 min)
1
3
5
6
7
10
0
20
40
60
80
100
120
140
160
180
200
220
1
2
3
4
5
6
10/21/10
10/22/10
10/23/10
10/24/10
10/25/10
10/26/10
10/27/10

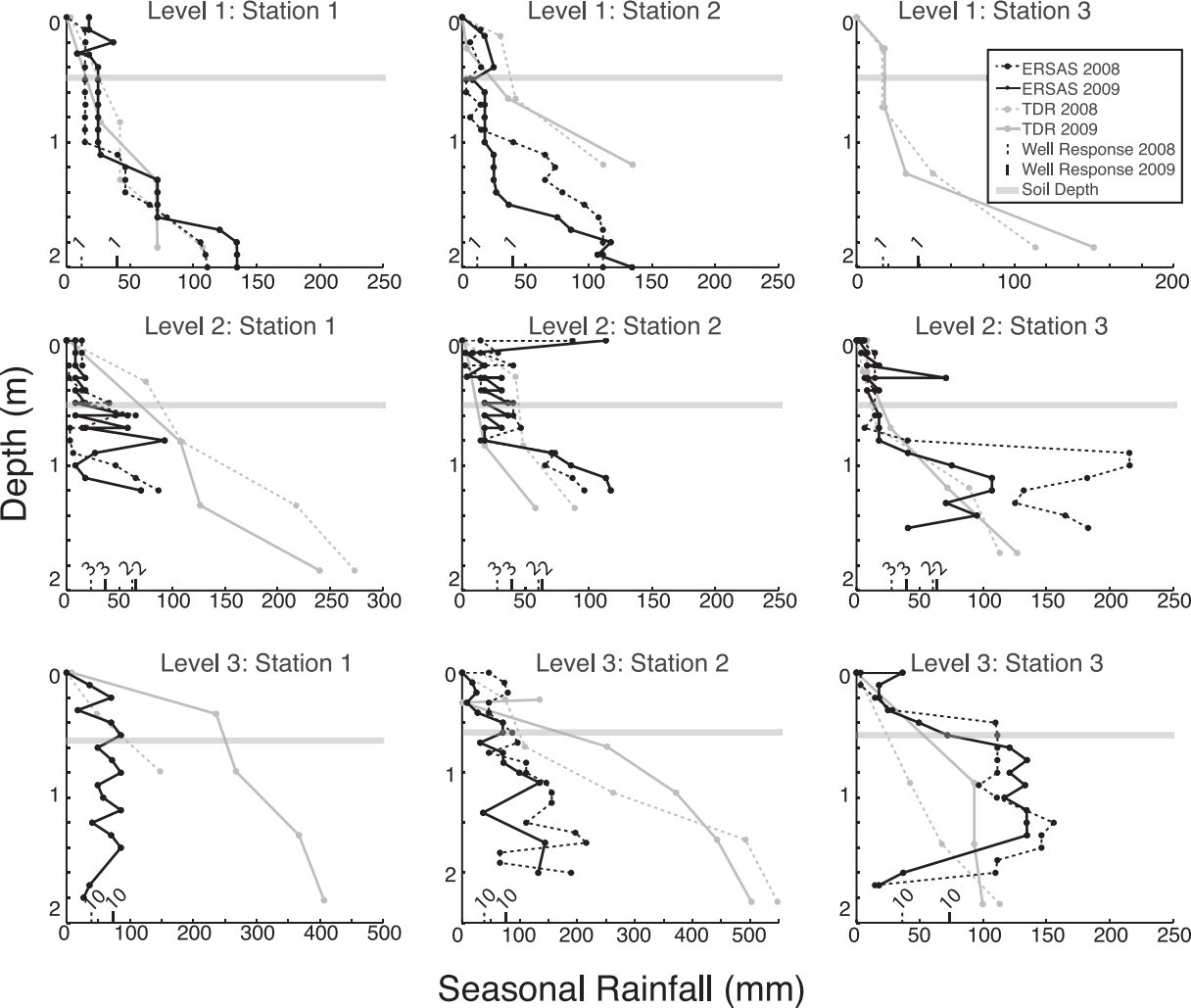
Level 1: Station 1
Level 1: Station 2
Level 1: Station 3
Level 2: Station 1
Level 2: Station 2
Level 2: Station 3
Level 3: Station 1
Level 3: Station 2
Level 3: Station 3
ERSAS 2008
ERSAS 2009
TDR 2008
TDR 2009
Well Response 2008
Well Response 2009
Soil Depth
Depth (m)
Seasonal Rainfall (mm)

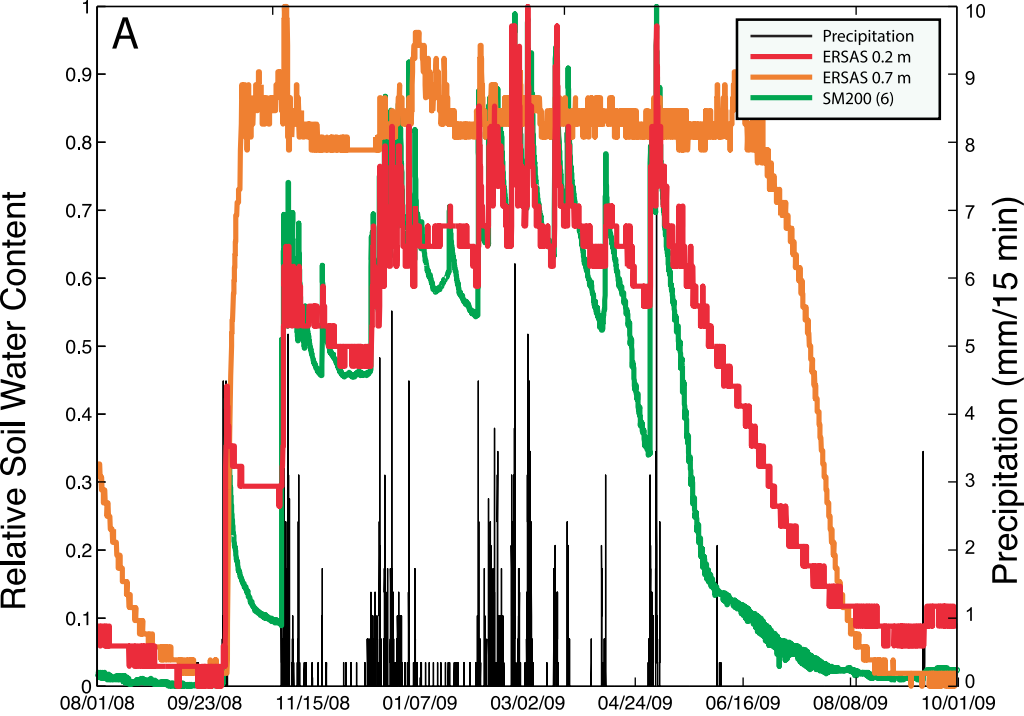
A
Precipitation
ERSAS 0.2 m
ERSAS 0.7 m
SM200 (6)
Relative Soil Water Content
Precipitation (mm/15 min)
0
0.1
0.2
0.3
0.4
0.5
0.6
0.7
0.8
0.9
1
0
1
2
3
4
5
6
7
8
9
10
08/01/08
09/23/08
11/15/08
01/07/09
03/02/09
04/24/09
06/16/09
08/08/09
10/01/09

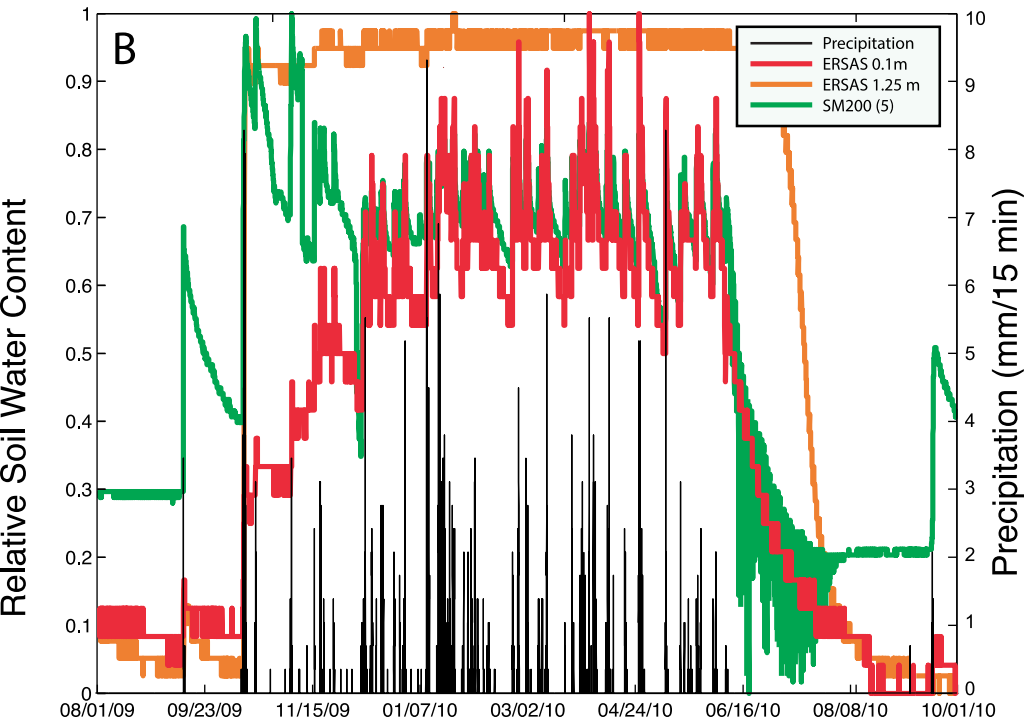
B
Precipitation
ERSAS 0.1m
ERSAS 1.25 m
SM200 (5)
Relative Soil Water Content
Precipitation (mm/15 min)
0
0.1
0.2
0.3
0.4
0.5
0.6
0.7
0.8
0.9
1
0
1
2
3
4
5
6
7
8
9
10
08/01/09
09/23/09
11/15/09
01/07/10
03/02/10
04/24/10
06/16/10
08/08/10
10/01/10

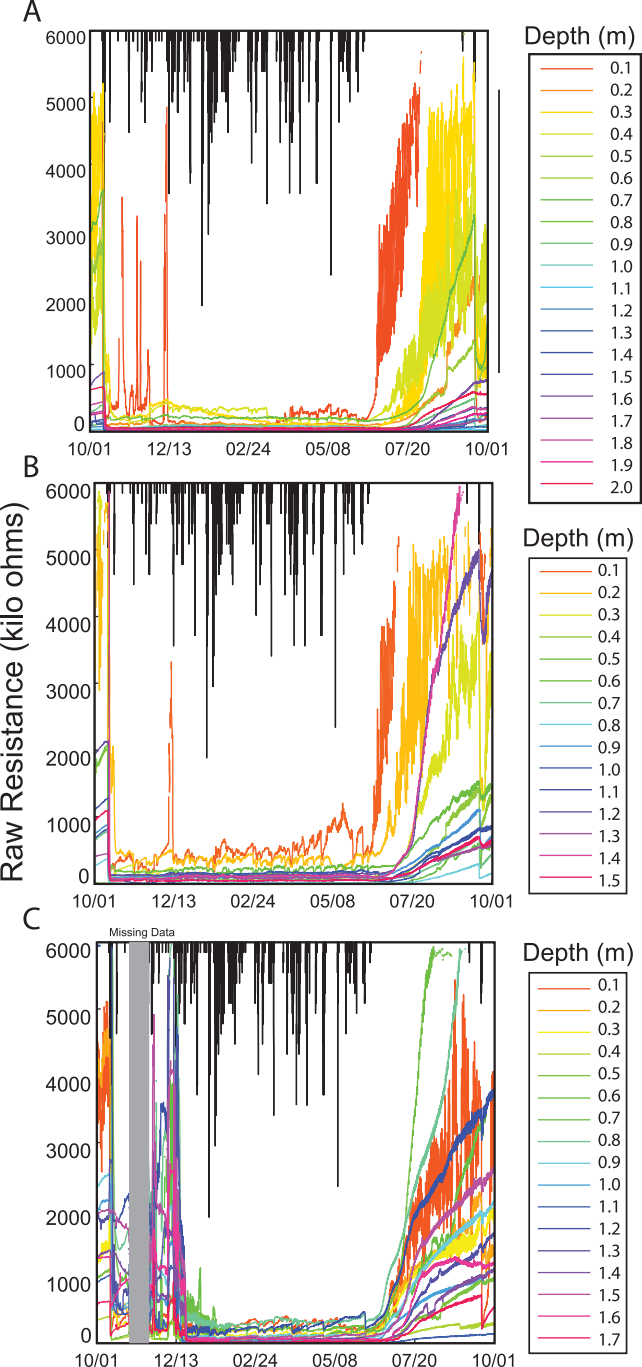
A
B
C
Raw Resistance (kilo ohms)
Missing Data
Depth (m)
0.1
0.2
0.3
0.4
0.5
0.6
0.7
0.8
0.9
1.0
1.1
1.2
1.3
1.4
1.5
1.6
1.7
1.8
1.9
2.0
0
1000
2000
3000
4000
5000
6000
10/01
12/13
02/24
05/08
07/20
10/01

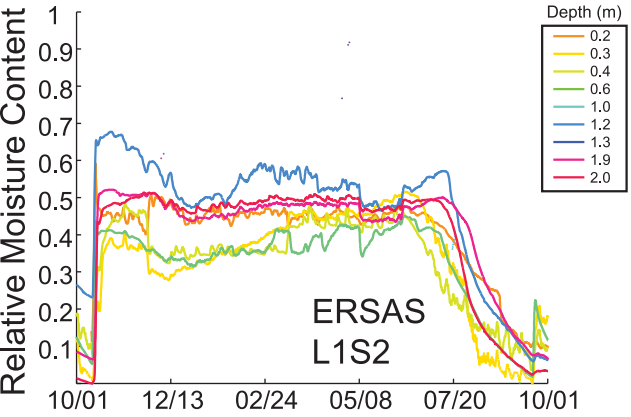
Relative Moisture Content
Depth (m)
0.2
0.3
0.4
0.6
1.0
1.2
1.3
1.9
2.0
ERSAS
L1S2
10/01
12/13
02/24
05/08
07/20
10/01

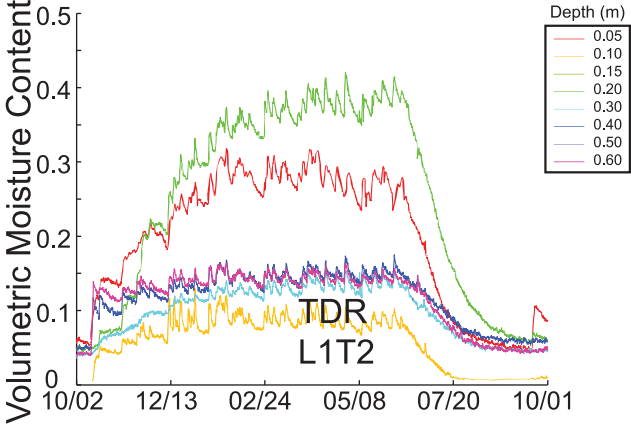
Volumetric Moisture Content
Depth (m)
0.05
0.10
0.15
0.20
0.30
0.40
0.50
0.60
TDR
L1T2
10/02
12/13
02/24
05/08
07/20
10/01

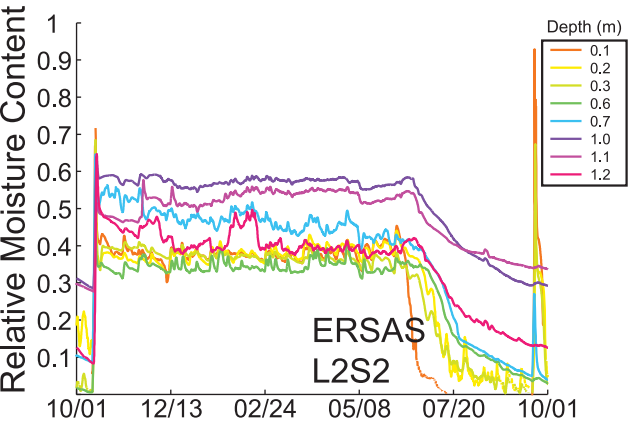
Relative Moisture Content
Depth (m)
0.1
0.2
0.3
0.6
0.7
1.0
1.1
1.2
ERSAS
L2S2
10/01
12/13
02/24
05/08
07/20
10/01

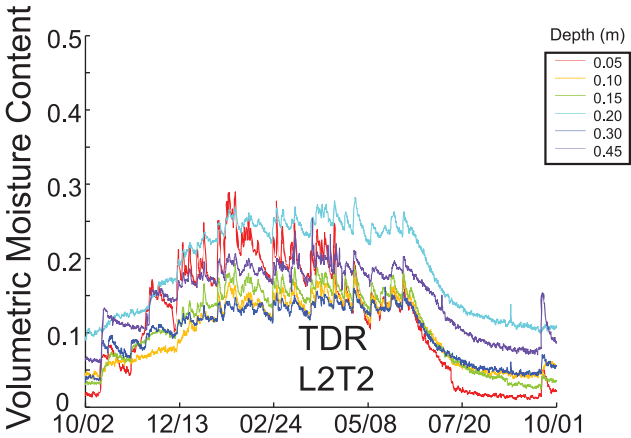
Volumetric Moisture Content
Depth (m)
0.05
0.10
0.15
0.20
0.30
0.45
TDR
L2T2
10/02
12/13
02/24
05/08
07/20
10/01

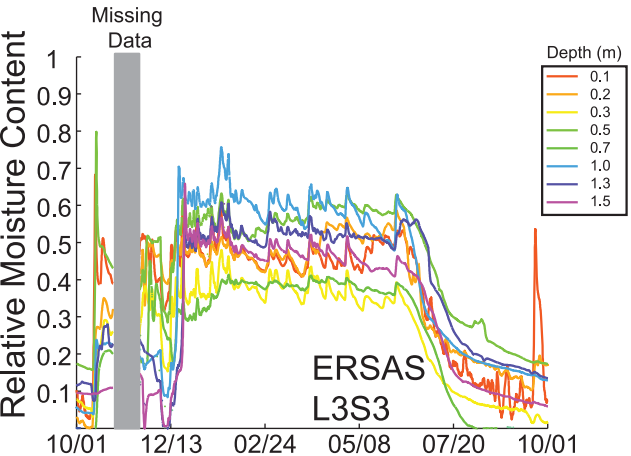
Missing
Data
Relative Moisture Content
Depth (m)
0.1
0.2
0.3
0.5
0.7
1.0
1.3
1.5
ERSAS
L3S3
10/01
12/13
02/24
05/08
07/20
10/01

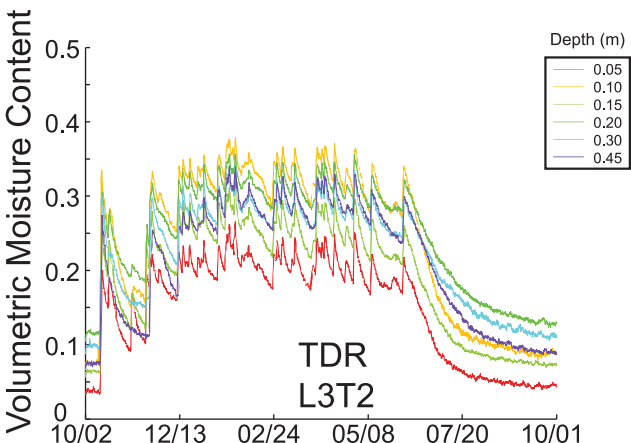
Volumetric Moisture Content
Depth (m)
0.05
0.10
0.15
0.20
0.30
0.45
TDR
L3T2
10/02
12/13
02/24
05/08
07/20
10/01

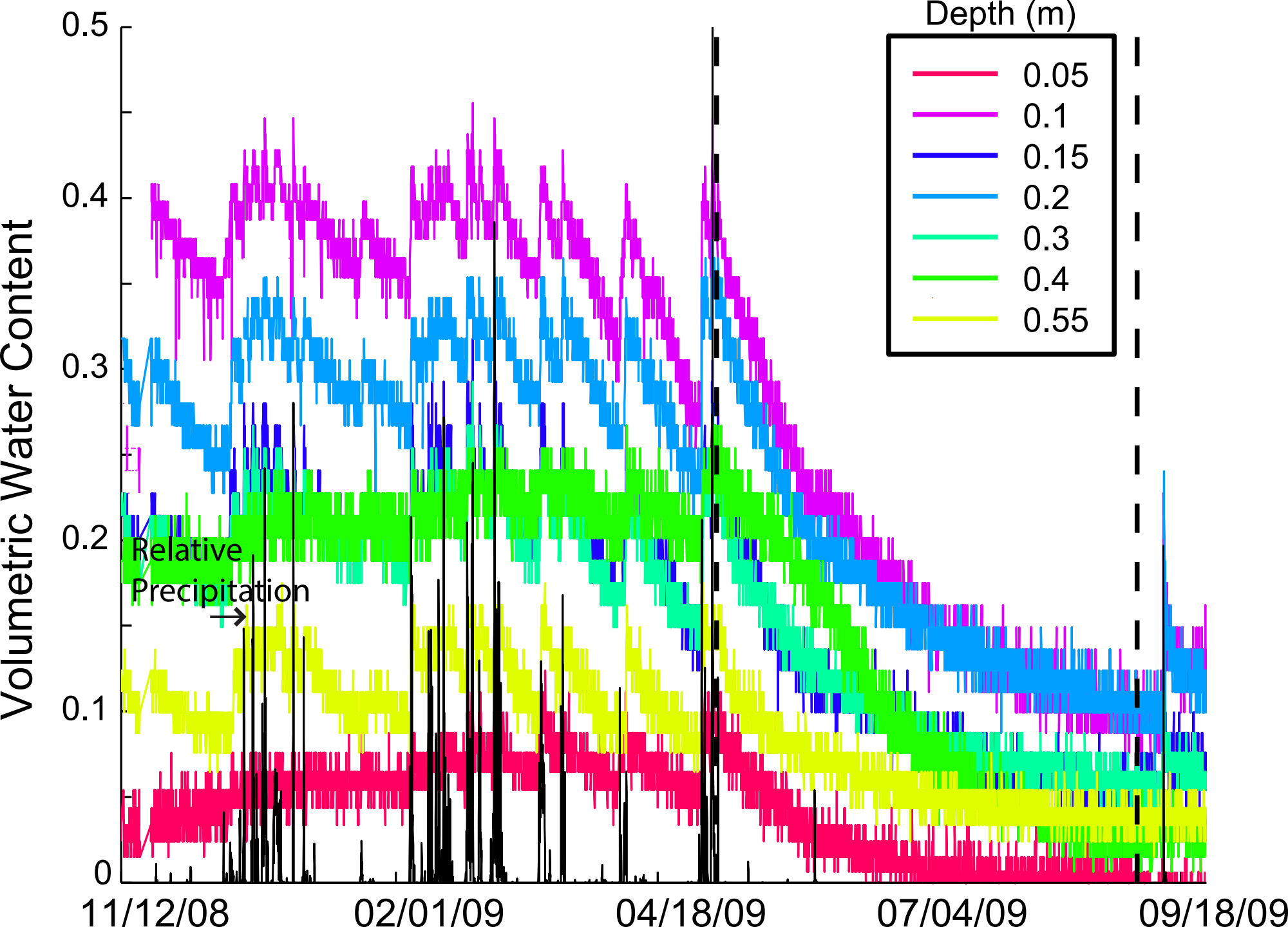
Depth (m)
0.05
0.1
0.15
0.2
0.3
0.4
0.55
Volumetric Water Content
0.5
0.4
0.3
0.2
0.1
0
Relative
Precipitation
11/12/08
02/01/09
04/18/09
07/04/09
09/18/09

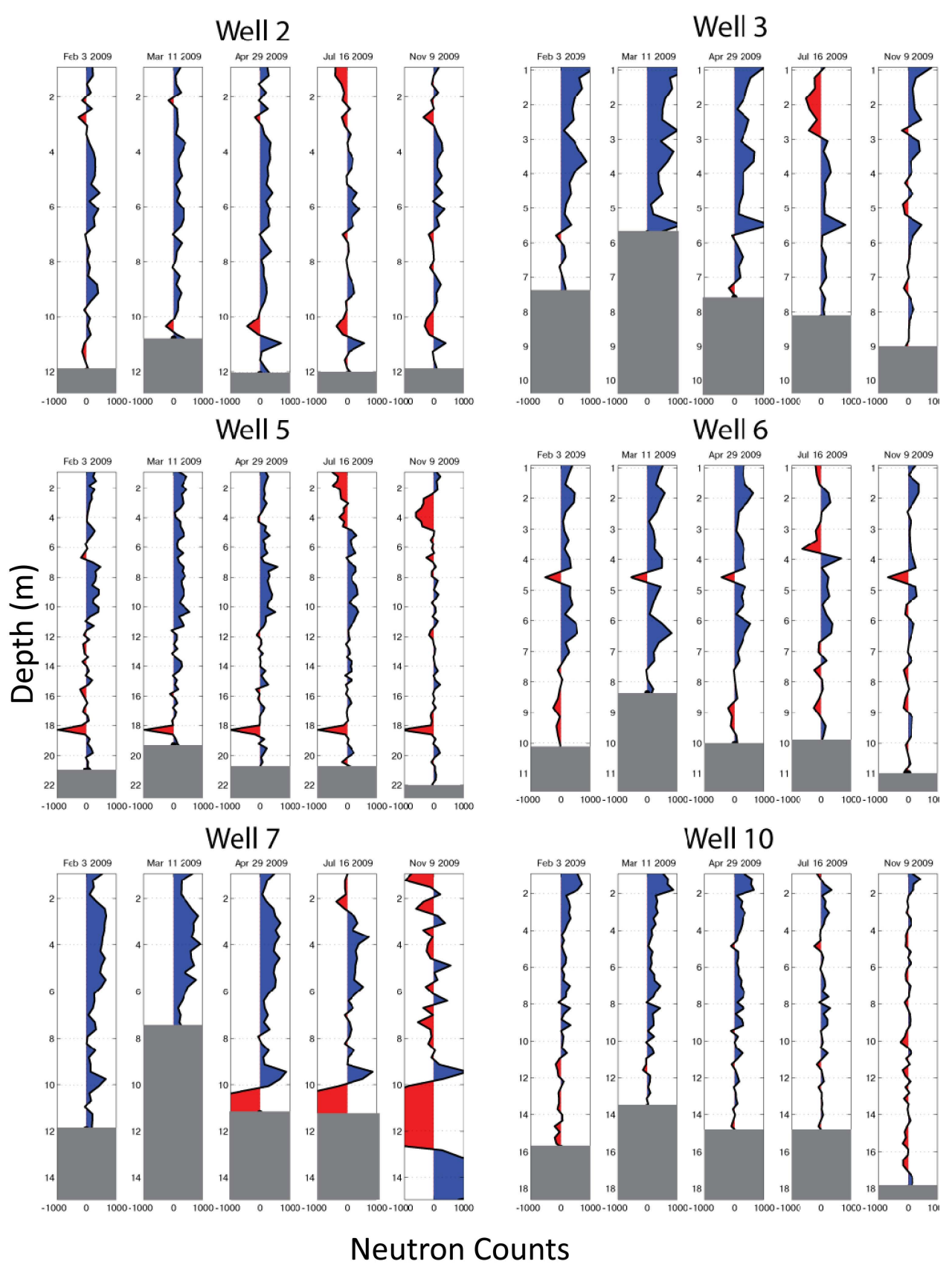
Well 2
Well 3
Well 5
Well 6
Well 7
Well 10
Feb 3 2009
Mar 11 2009
Apr 29 2009
Jul 16 2009
Nov 9 2009
Depth (m)
Neutron Counts

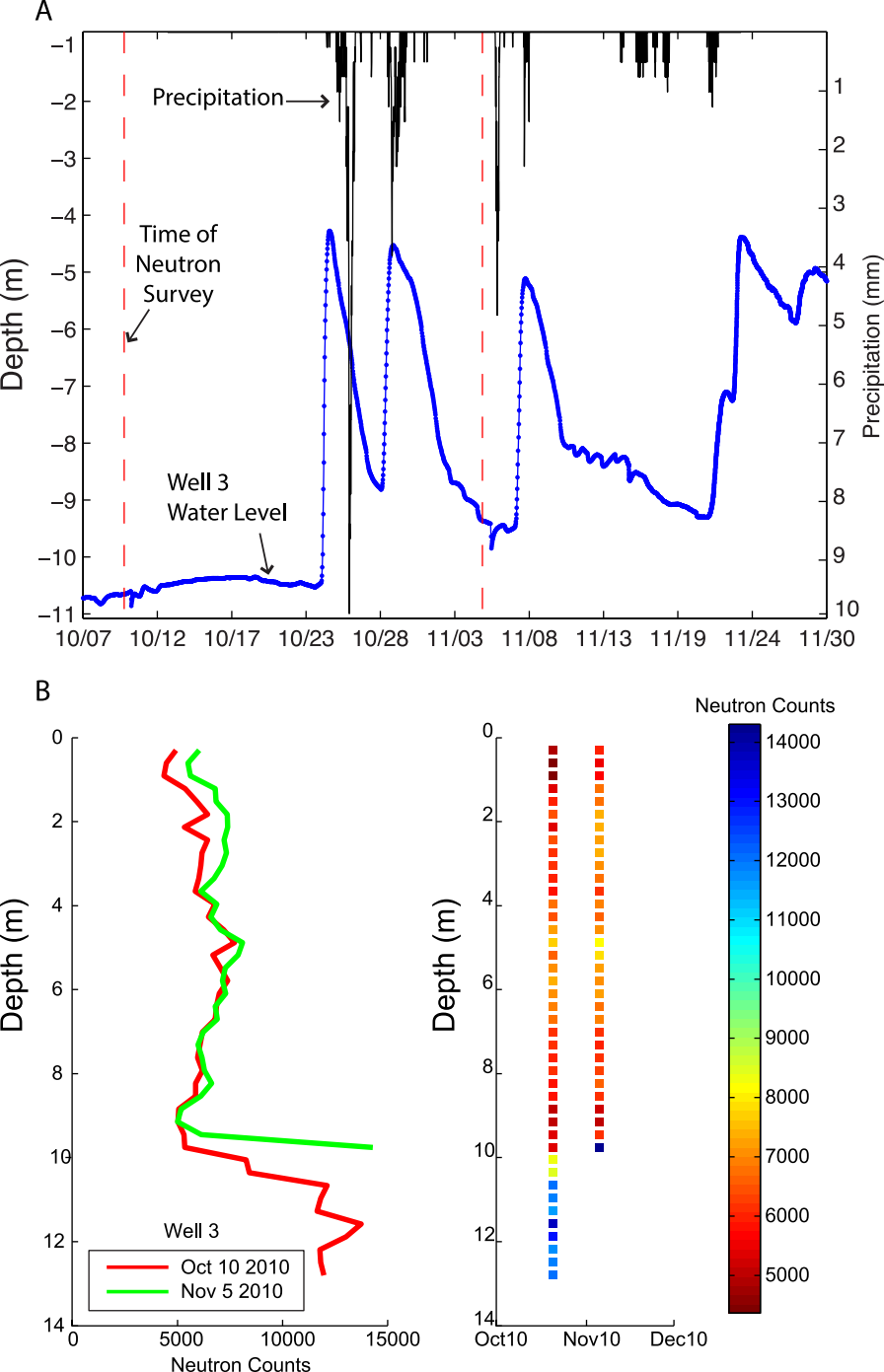
A
Precipitation
Time of
Neutron
Survey
Well 3
Water Level
Depth (m)
Precipitation (mm)
10/07
10/12
10/17
10/23
10/28
11/03
11/08
11/13
11/19
11/24
11/30
B
Well 3
Oct 10 2010
Nov 5 2010
Depth (m)
Neutron Counts
Oct10
Nov10
Dec10
Neutron Counts

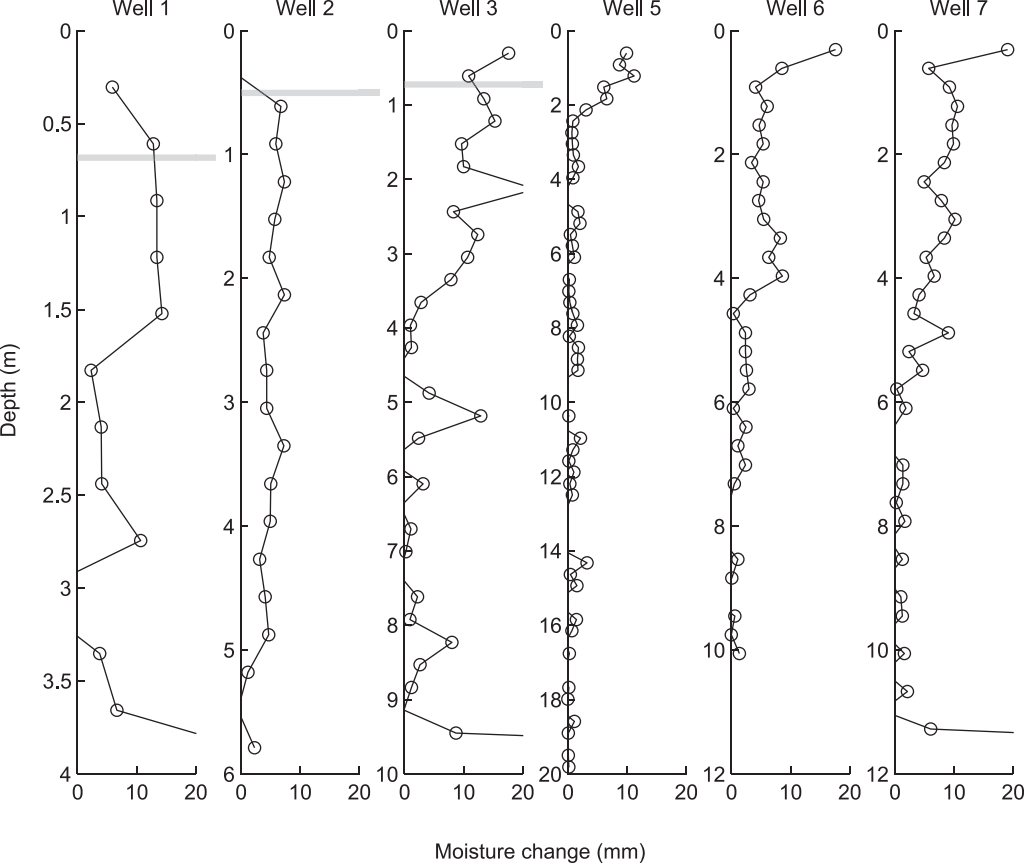
Well 1
Well 2
Well 3
Well 5
Well 6
Well 7
Depth (m)
Moisture change (mm)

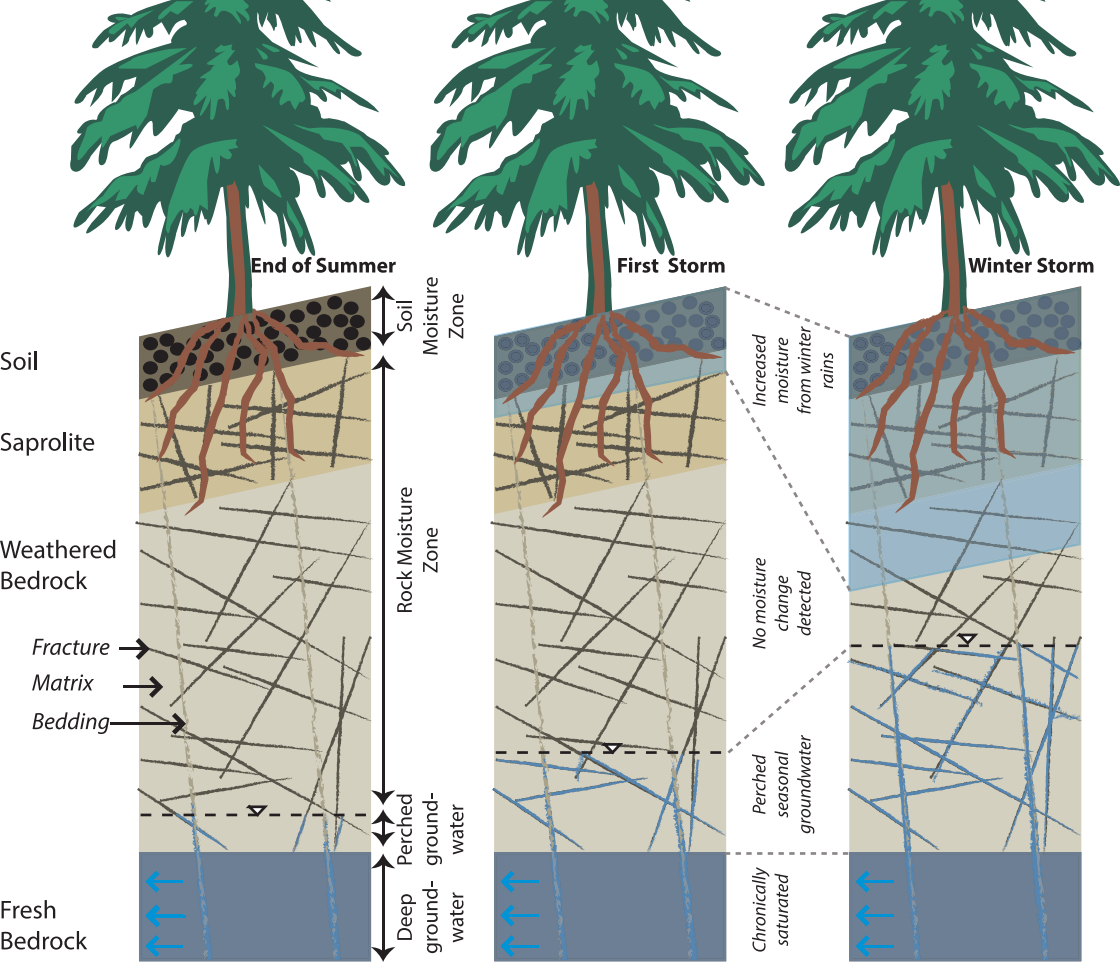
End of Summer
First Storm
Winter Storm
Soil
Saprolite
Weathered Bedrock
Fresh Bedrock
Fracture
Matrix
Bedding
Soil Moisture Zone
Rock Moisture Zone
Perched ground-water
Deep ground-water
Increased moisture from winter rains
No moisture change detected
Perched seasonal groundwater
Chronically saturated